Astrophysics with ultra-high energy cosmic rays

Lorenzo Caccianiga for the Pierre Auger Collaboration

IASF - Milano 29/1/2020

Ultra-high energy cosmic rays

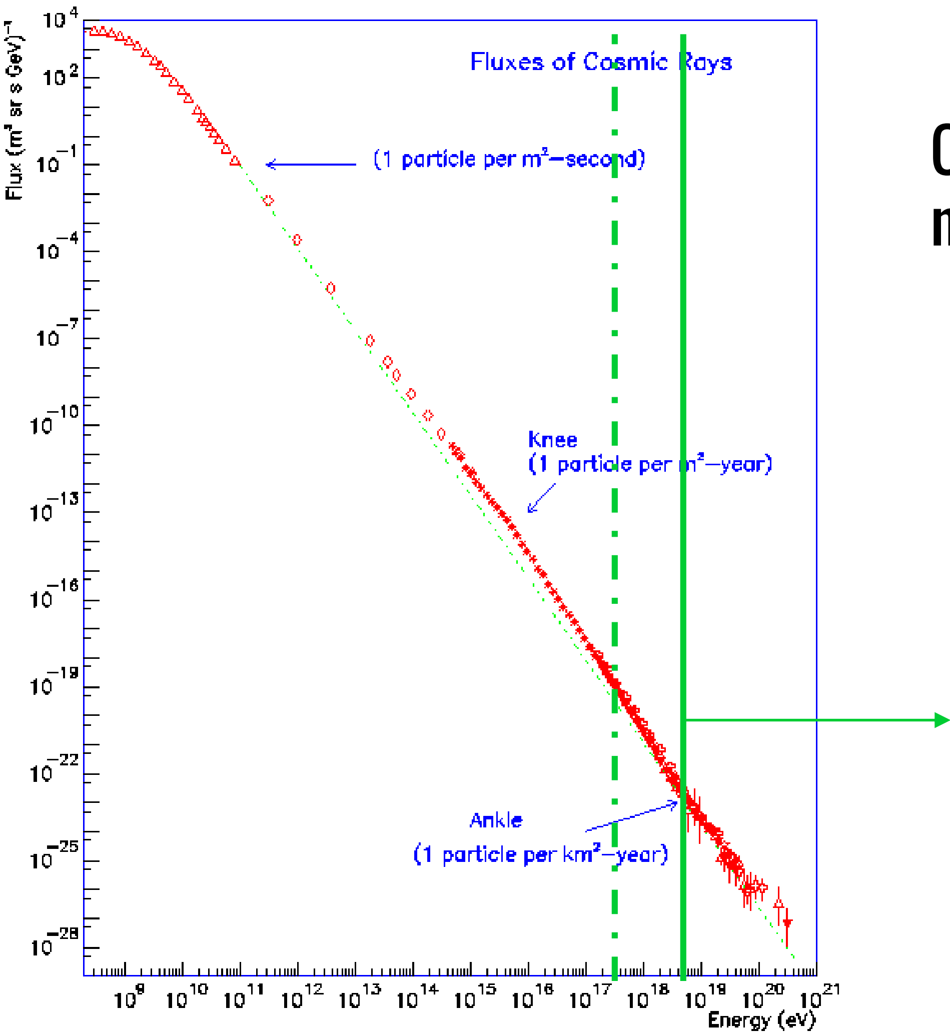

Charged particles, mainly protons and nuclei up to Iron

- Understand the end of the CR spectrum
- Exploit the highest energy events for anisotropy studies
- Study particle interactions at energies higher than the ones accessible by accelerators

UHECR propagation - GZK

Greisen-Zatsepin-Kuz'min - **GZK effect** (1966)

$$\gamma_{2.7\,\mathrm{K}} + p \rightarrow \Delta^{+} \rightarrow n + \pi^{+} or \;\; p + \pi^{0}$$

$$\gamma_{\mathrm{IR}/2.7\,\mathrm{K}} + A \rightarrow (A-1) + n$$

- Implication: sources should lie within ~100 Mpc at 10^{20} eV
- Neutrinos produced by the decay of π^{+} and n
- Photons resulting from the decay of π^{0}

UHECR propagation - Magnetic Fields

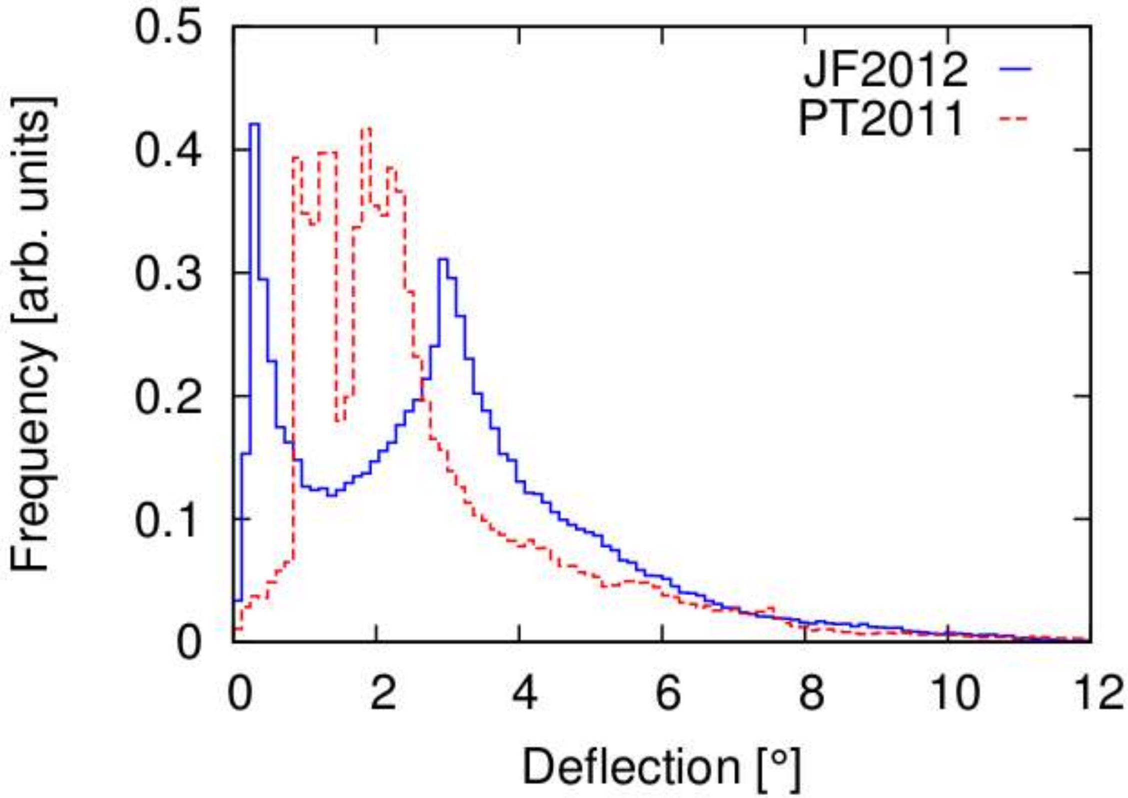

Figure 3. Distribution of UHECR deflections in two Galactic magnetic field models marked PT2011 [44] and JF2012 [45] for the regular component. The energies of actual UHECRs are renormalized to show the distributions for $E/Z = 100\,\mathrm{EeV}$. The double-peak structure is mostly due to the fact that UHECRs from different Galactic hemispheres undergo different deflections.

Candidate sources

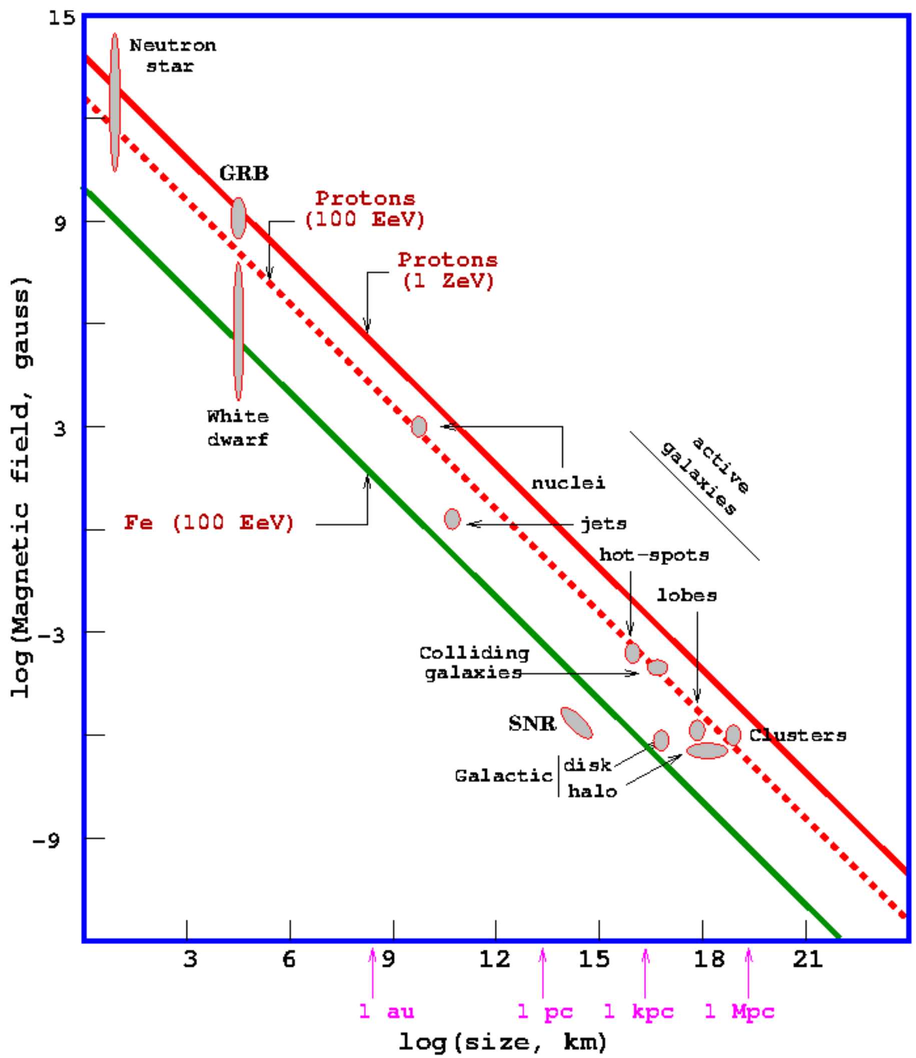

All acceleration models require the cosmic ray to be confined into the source.
➔ stringent conditions on the magnetic fields of the candidate sources

$$E_{max}^{Limit} \mu\ Z \times L \times B$$

Extensive Air Showers

When a UHECR interact with the high atmosphere, it creates a cascade of secondary particles: an extensive air shower (EAS)

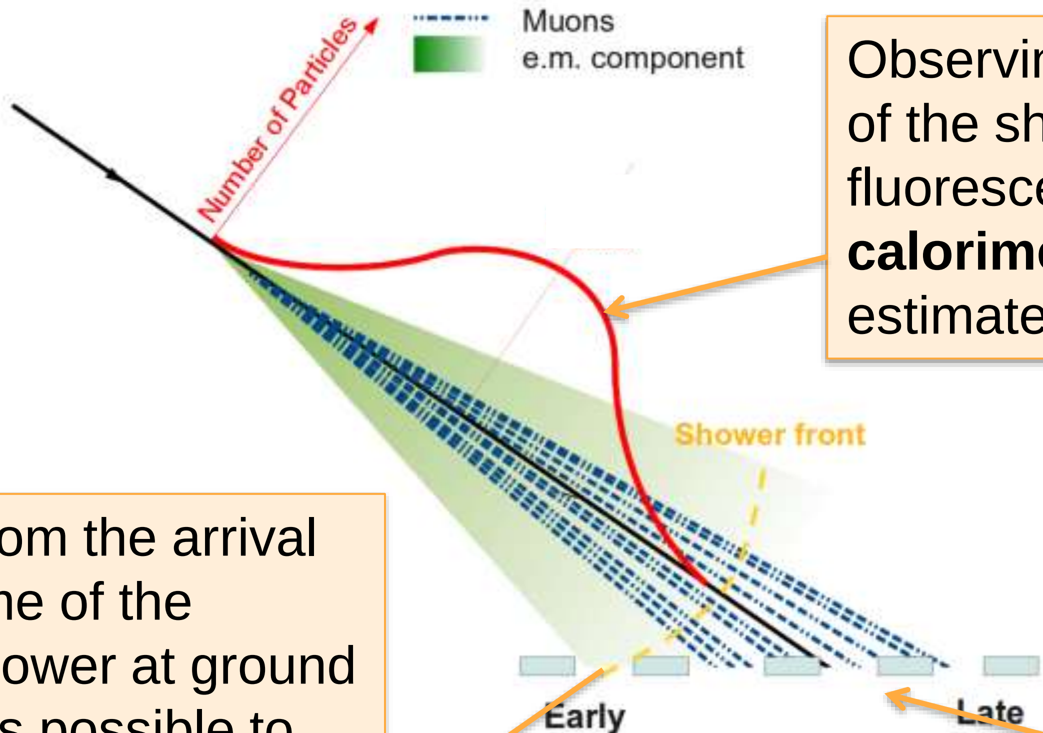

Observing the longitudinal profile of the shower (e.g. with fluorescence telescopes) the **total calorimetric energy** can be estimated

From the arrival time of the shower at ground it is possible to reconstruct the **arrival direction** of the primary

The number of particles at ground at a reference distance from the shower axis is a good **energy** estimator.
Needs to be absolutely calibrated:

- Monte Carlo
- Calorimetric measurements

The Pierre Auger Observatory

~400 collaborators
110 institutions from 17 countries

Argentina - Australia - Brazil - Colombia - Czech Republic - France - Germany - Italy - Mexico - Netherlands - Poland - Portugal - Romania - Slovenia - Spain - United Kingdom - United States

The Pierre Auger Observatory

Auger science case: "The Pierre Auger Observatory[. . .] employing a giant array of particle counters and an optical fluorescence detector[. . .] aims at studying, with high statistics, cosmic rays with energies around and above the so-called Greisen-Zatsepin-Kuzmin spectral cutoff[. . .] Its main aims are:[. . .]

1. a precise reconstruction of the energy spectrum...
2. the identification of primaries, even if only statistical...Are they protons, nuclei, or perhaps something exotic? (e.g., the detection of a large amount of gammas and neutrinos would be an
indication in favor of "exotic" theories...)...Inferences on mass composition will be drawn from the study of shower properties that might constrain hadronic interaction models at energies well beyond the reach of accelerator-based experiments...
3. a systematic study of the arrival directions, that will indicate if there is anisotropy in the distribution and/or clusters which would indicate the existence of point sources...

The Pierre Auger Observatory

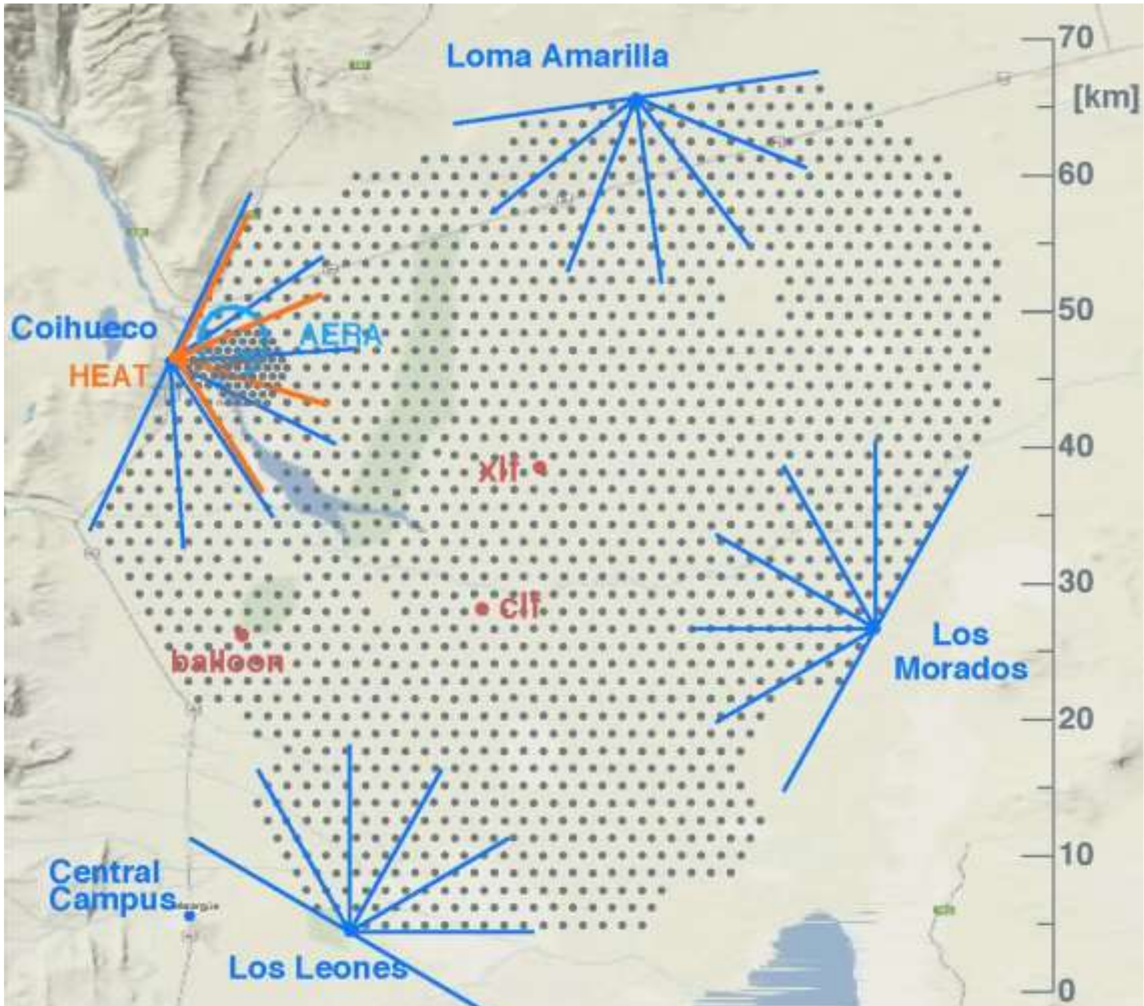

Data taking started in 2004, completed in 2008

Surface detector (SD) 1600 water Cherenkov detectors
1.5 km spacing
~3000 km^2

Fluorescence detector (FD)
24 UV telescopes

Enhancements
- low energy extension
- Buried muon detectors in some SD stations

The Pierre Auger Observatory

Each SD station is a tank filled with 12 t of ultra-pure water overlooked by 3 PMTs that measure the Cherenkov light produced by the particle of the shower.

The Pierre Auger Observatory

The **FD** measures the longitudinal profile and thus the total calorimetric energy (and also X_{max}).
But it only operates in clear moonless nights (~10% duty cycle)

→Energy calibration using **hybrid** events

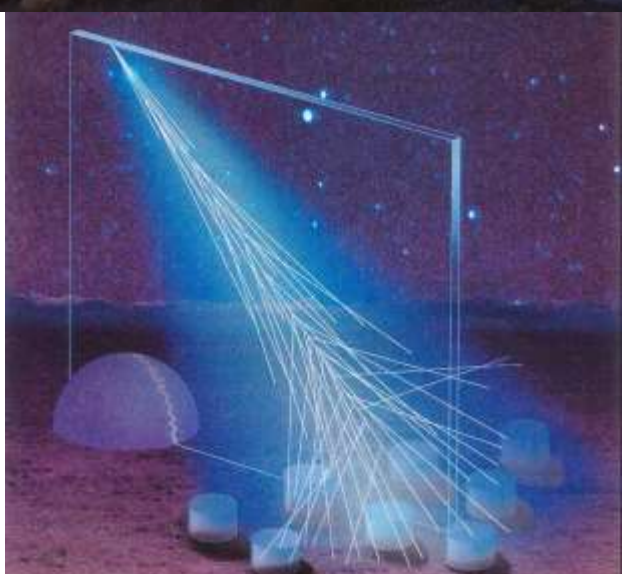

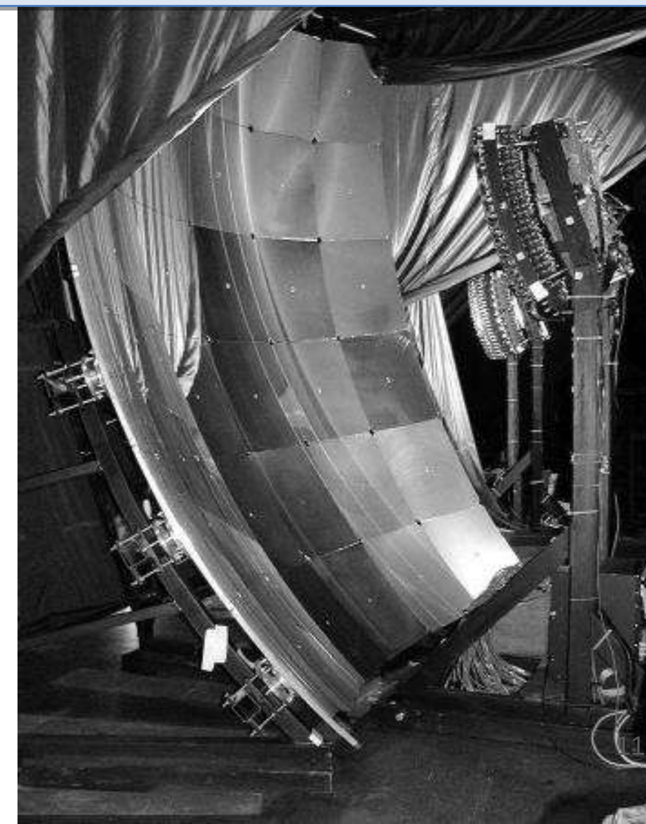

The Pierre Auger Observatory

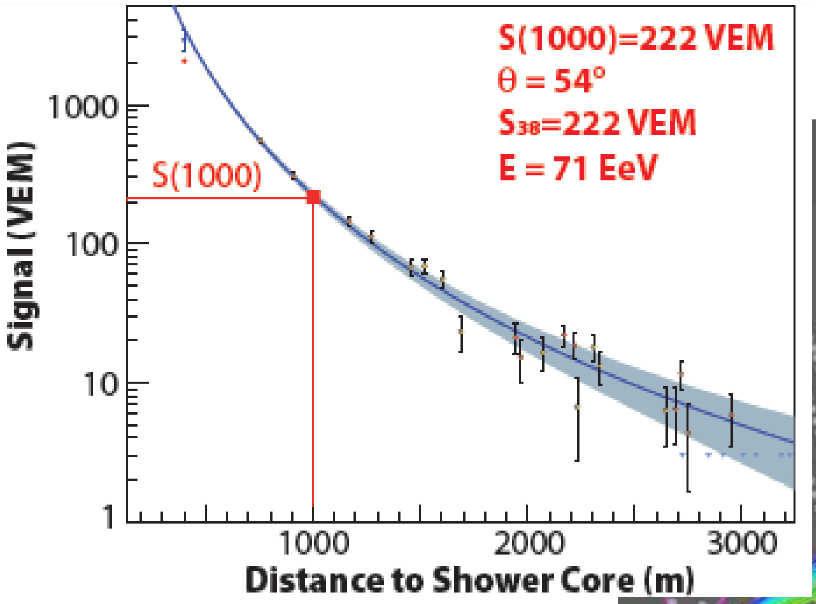

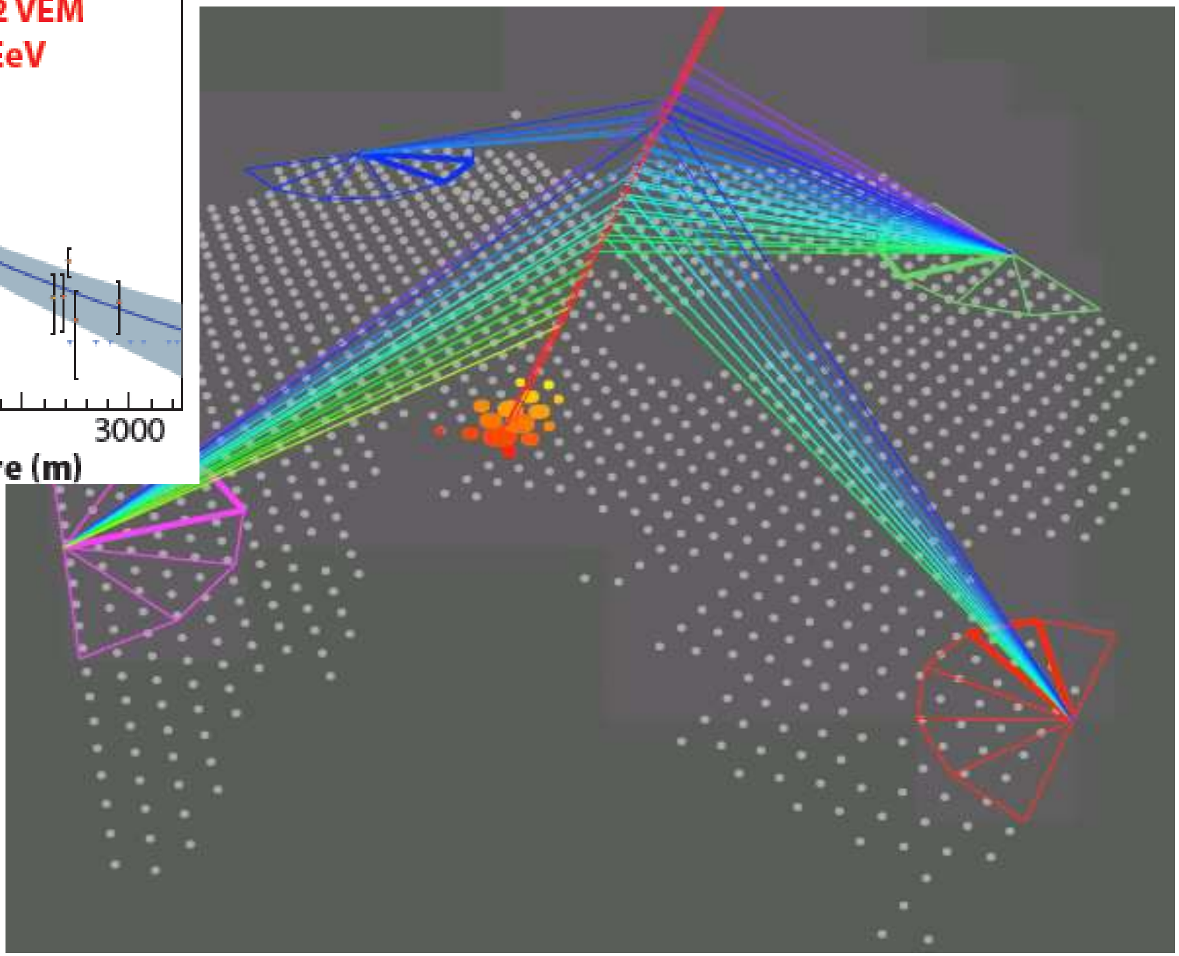

The Pierre Auger Observatory

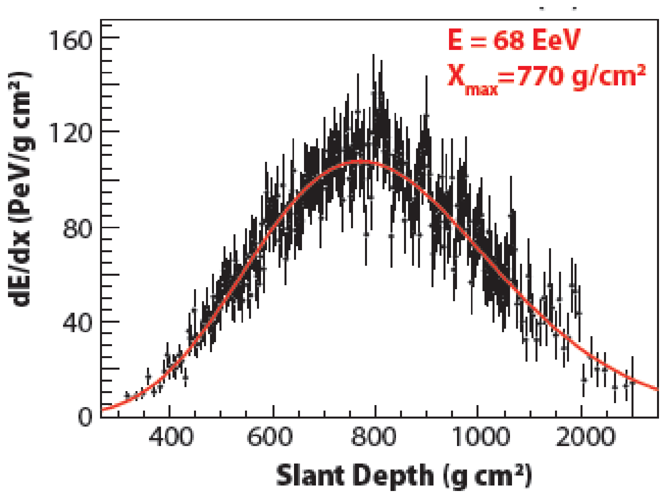

E Measured by FD

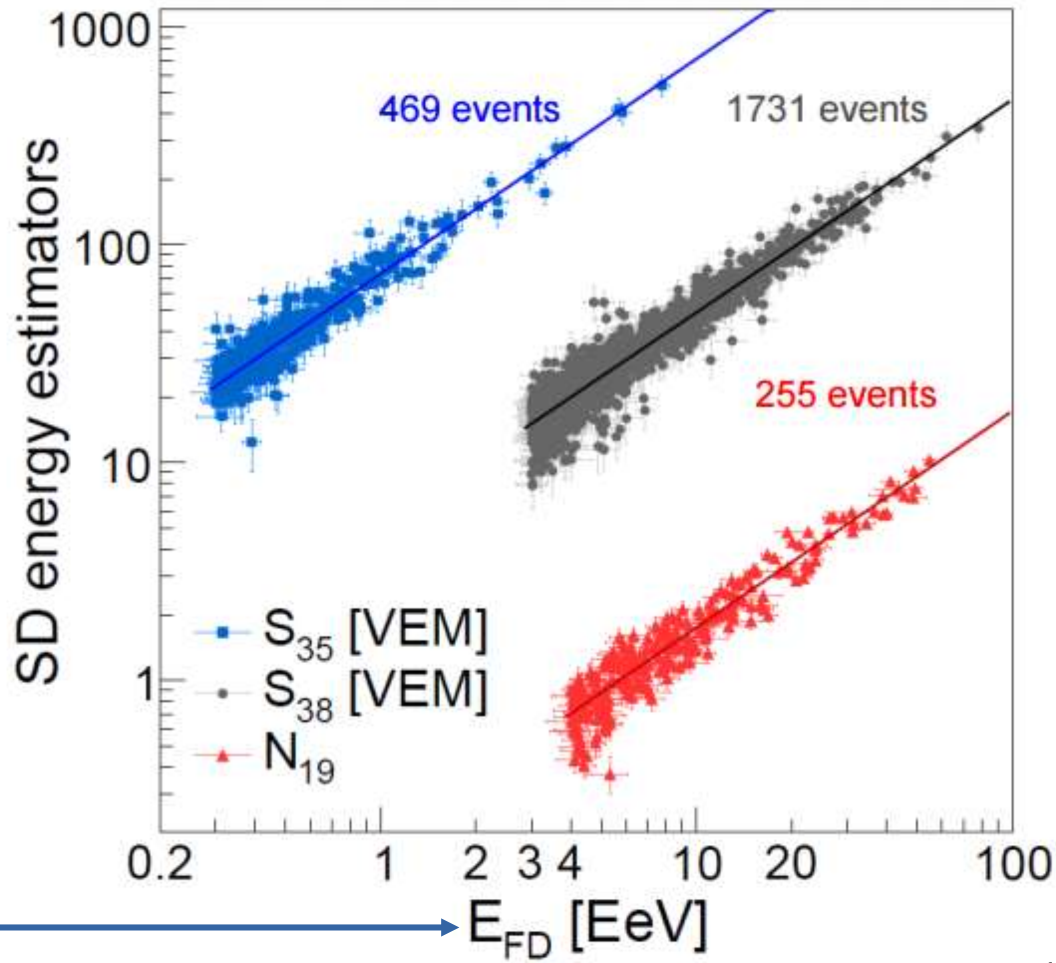

Energy spectrum

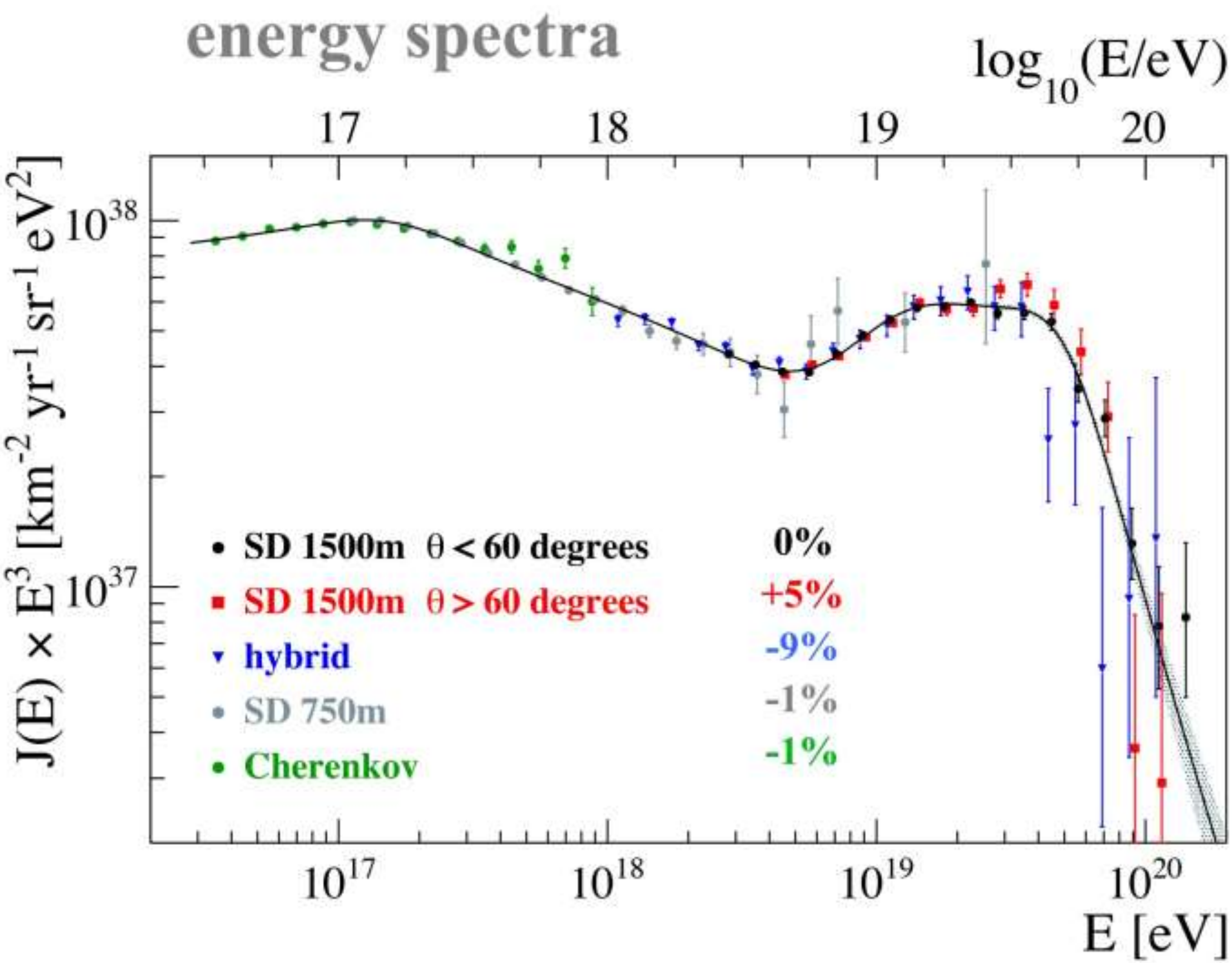

V. Verzi for the Pierre Auger Collaboration - ICRC 2019

Energy spectrum (2019)

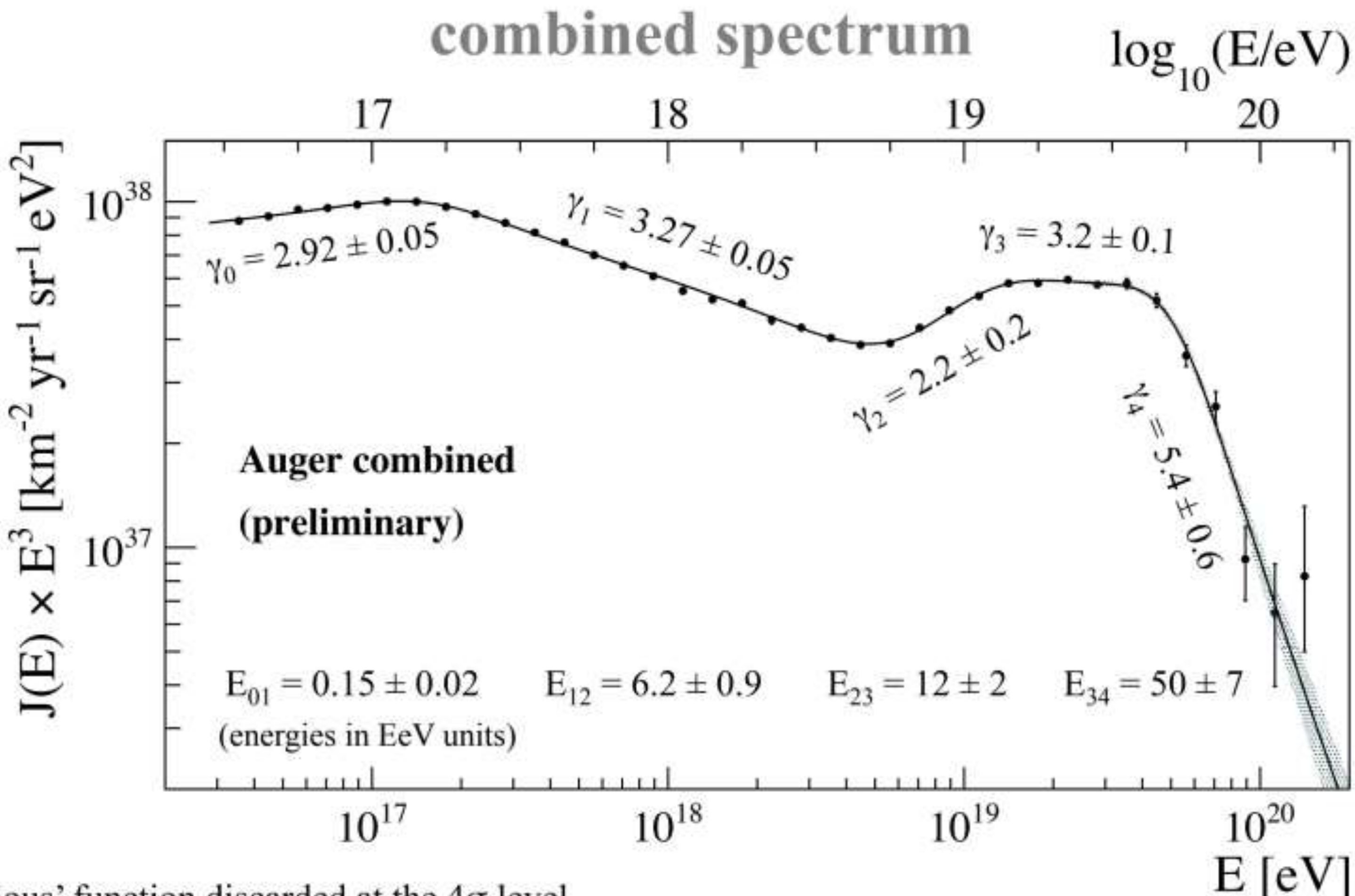

'previous' function discarded at the 4σ level

V. Verzi for the Pierre Auger Collaboration - ICRC 2019

Energy spectrum (2017)

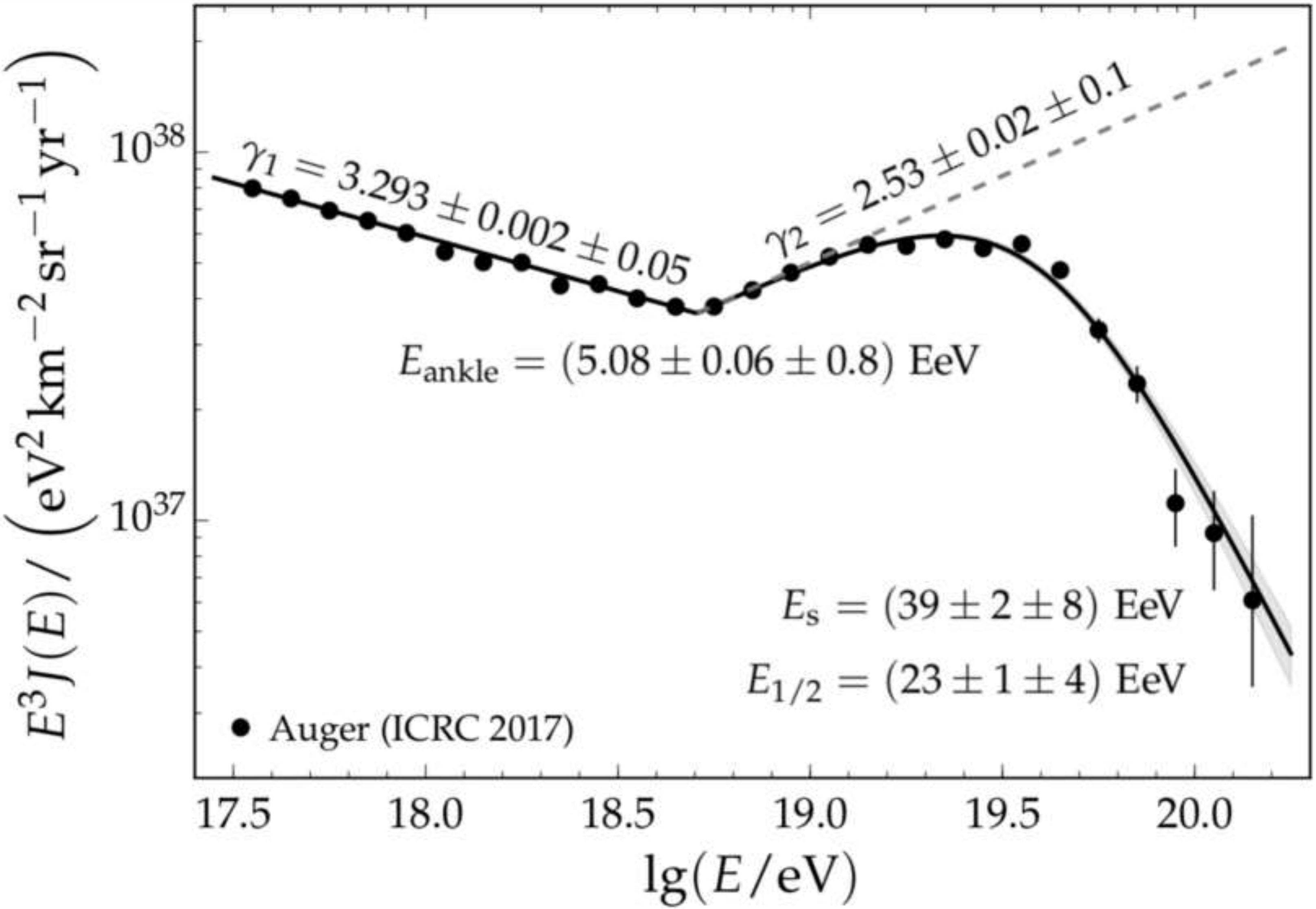

J. Bellido for the Pierre Auger Collaboration - ICRC 2017

Energy spectrum - comparison with TA

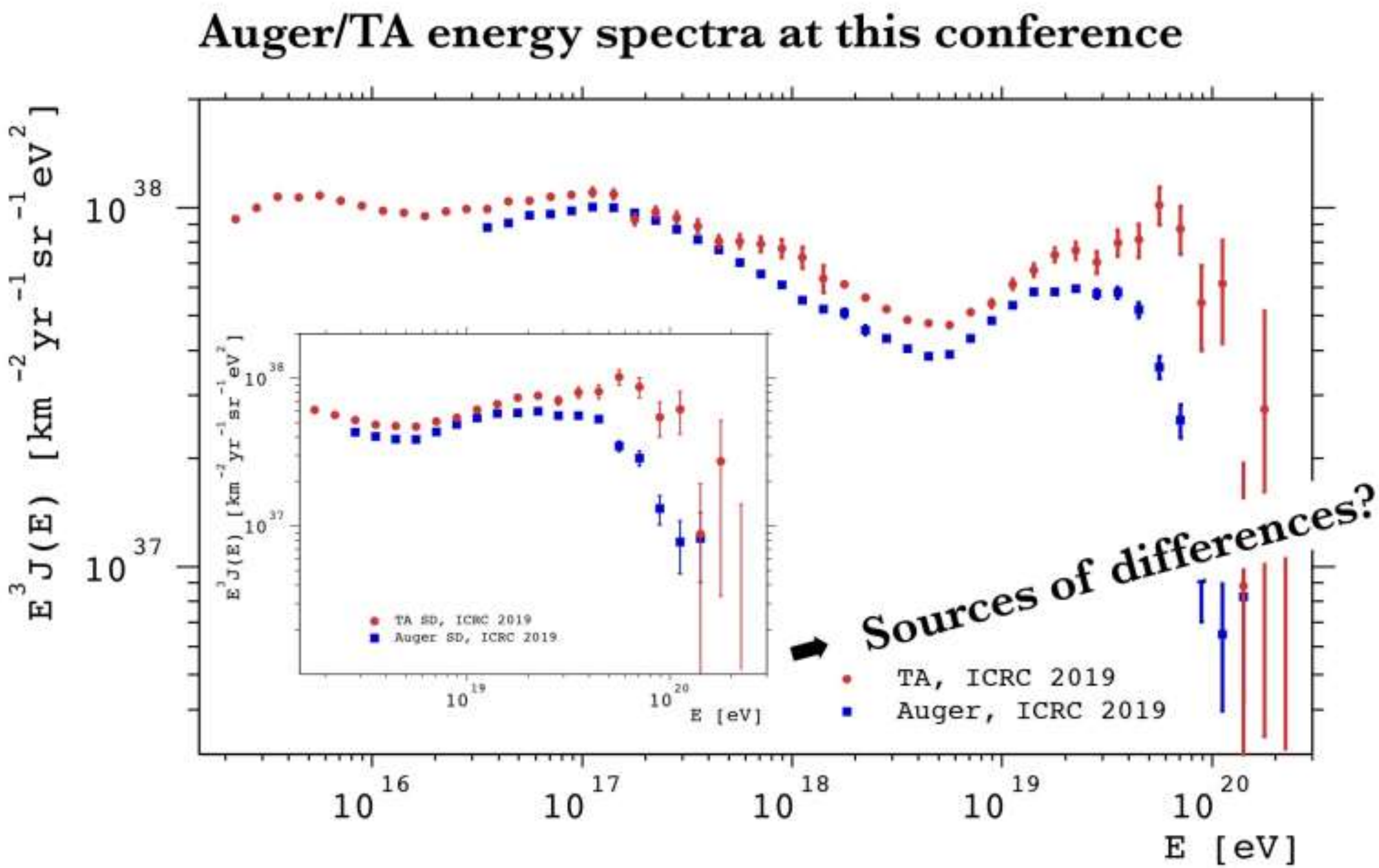

Composition

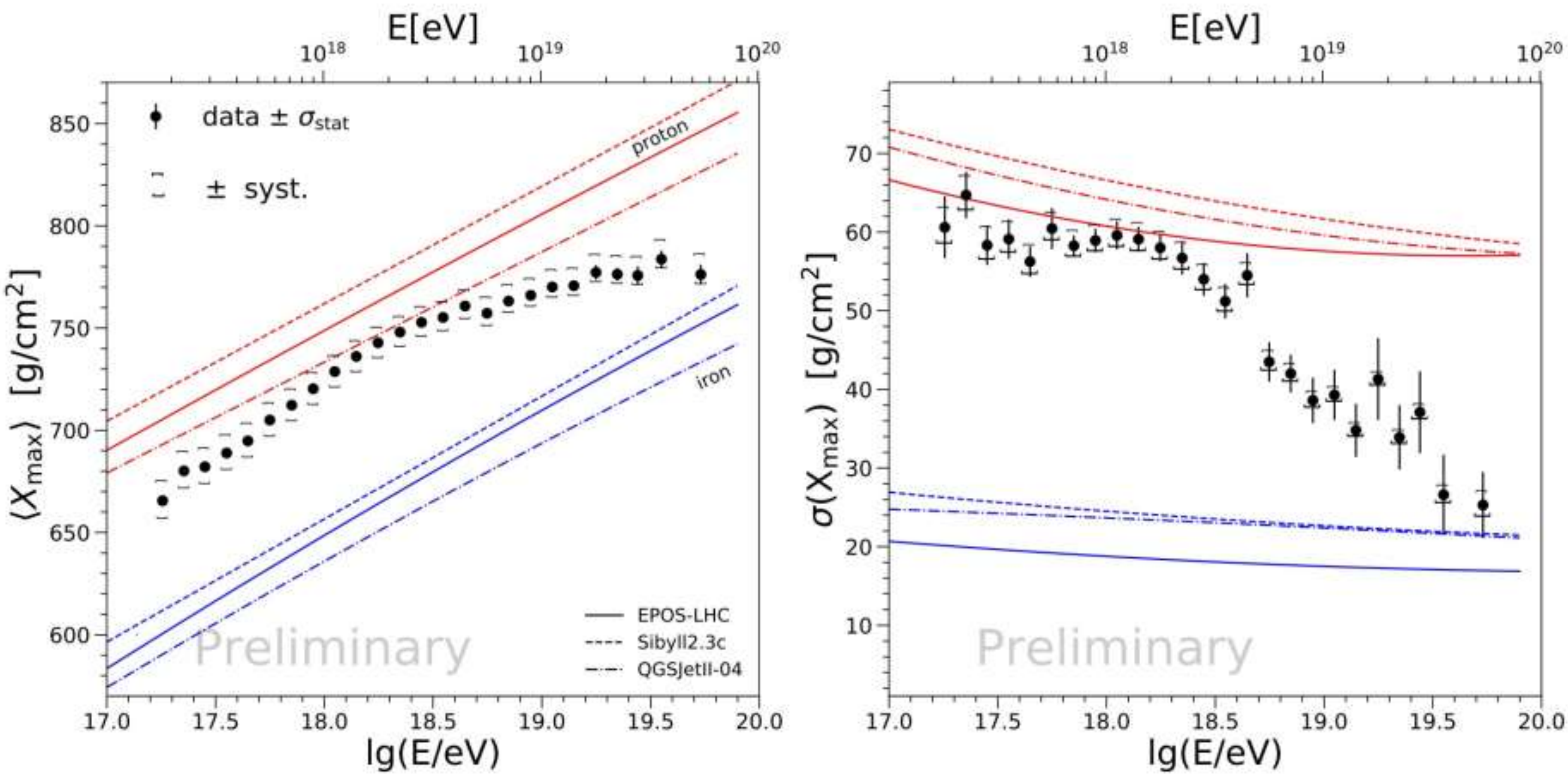

A. Yushkov for the Pierre Auger Collaboration - ICRC 2019

Composition and Hadronic interactions

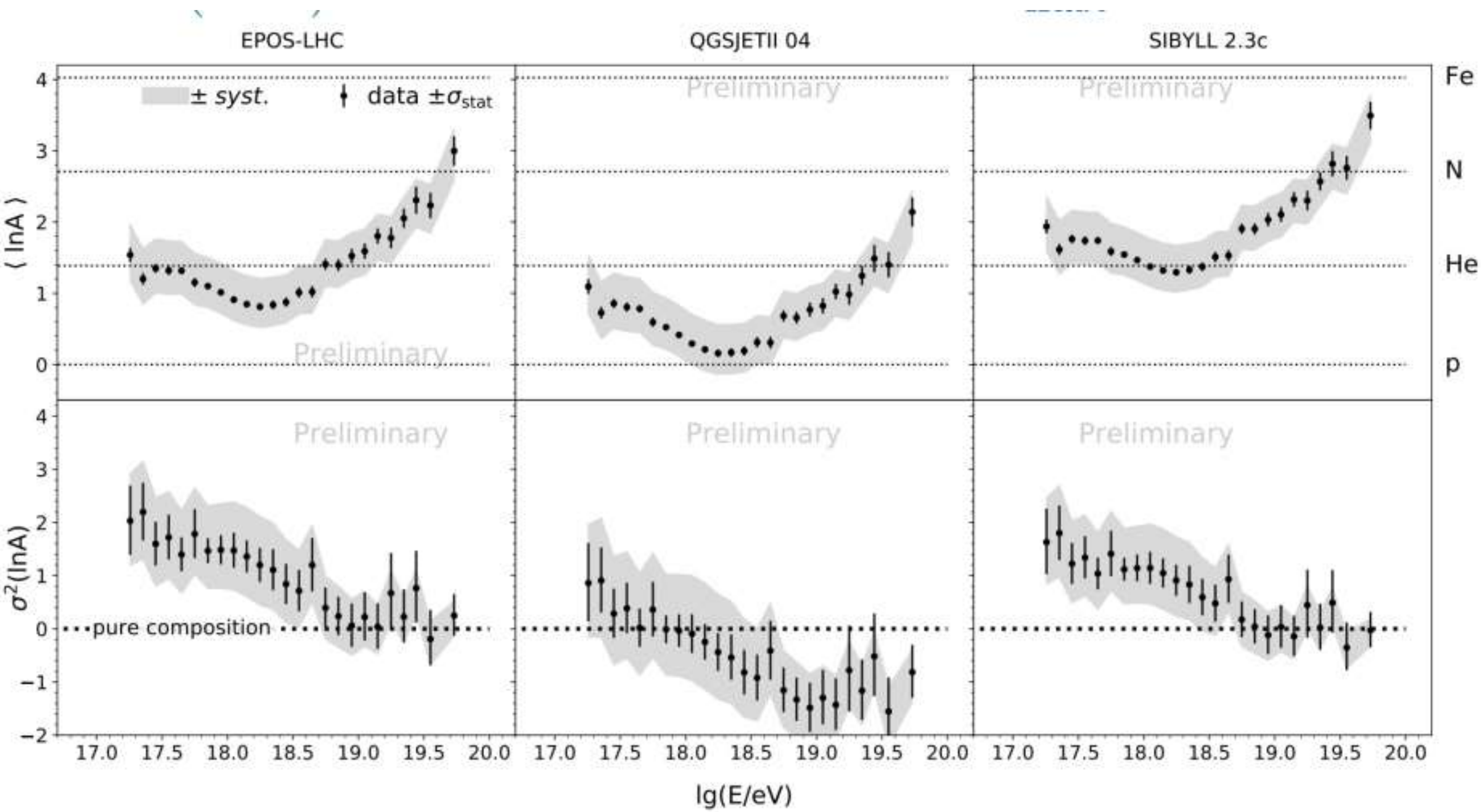

A. Yushkov for the Pierre Auger Collaboration - ICRC 2019

Composition and Hadronic interactions

M.Mallamaci for the Pierre Auger Collaboration - ICRC 2017

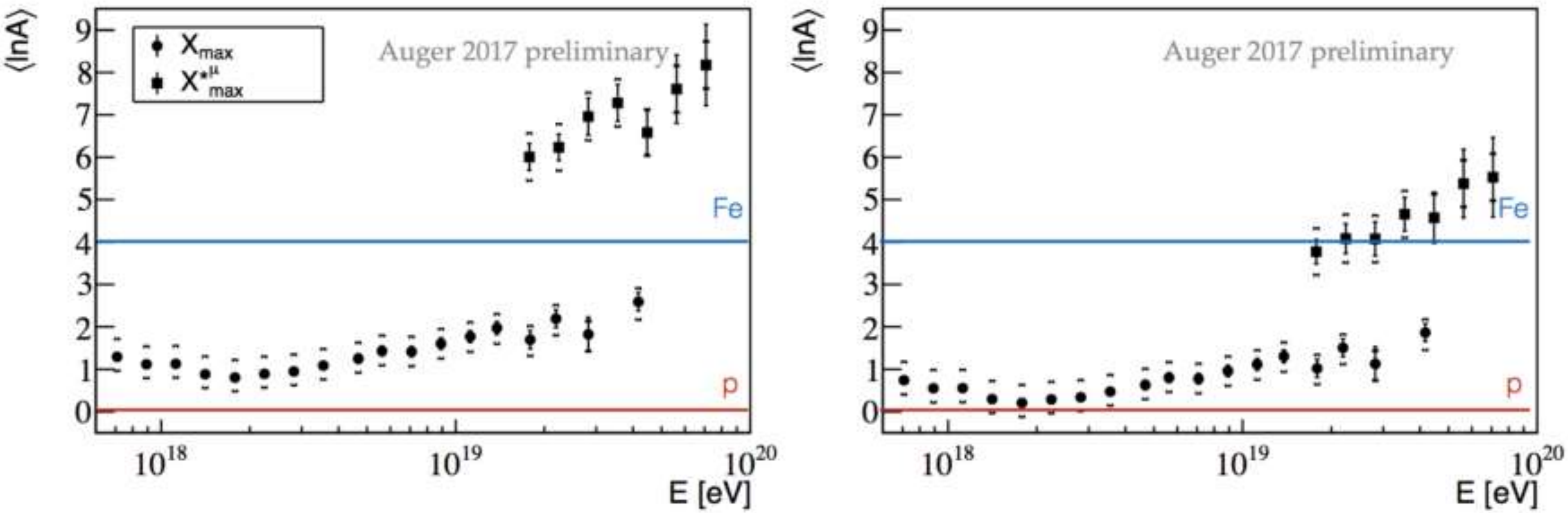

Figure 4: The evolution with energy of $\langle \ln A \rangle$ as obtained from the measured $X^{*\mu}_{\rm max}$ (squares). The results obtained for $X_{\rm max}$ (dots) [2] are also shown. EPOS-LHC (left) and QGSJetII-04 (right) are used as reference models. Square brackets correspond to the systematic uncertainties.

Composition and Hadronic interactions

F. Sanchez for the Pierre Auger Collaboration - ICRC 2019

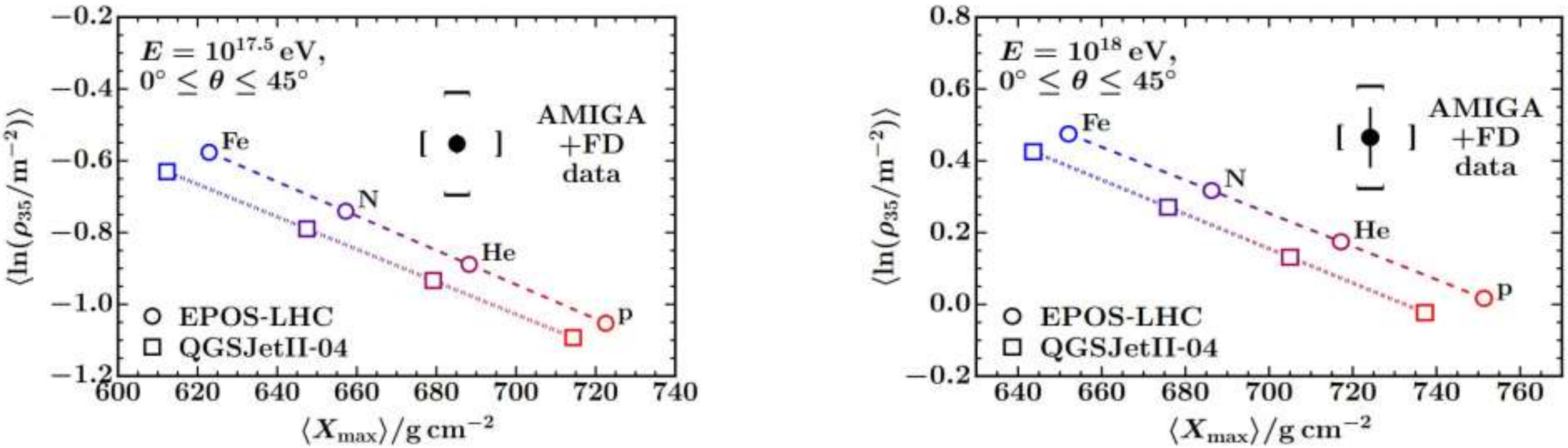

Take home message: no hadronic interaction model currently describes ultra-high energy showers properly

Large scale anisotropies

Results published in Science 2017: dipole observed for E>8 EeV data, no anisotropy in 4-8 EeV data

THE ASTROPHYSICAL JOURNAL, 868:4 (12pp), 2018 November 20 Aab et al.

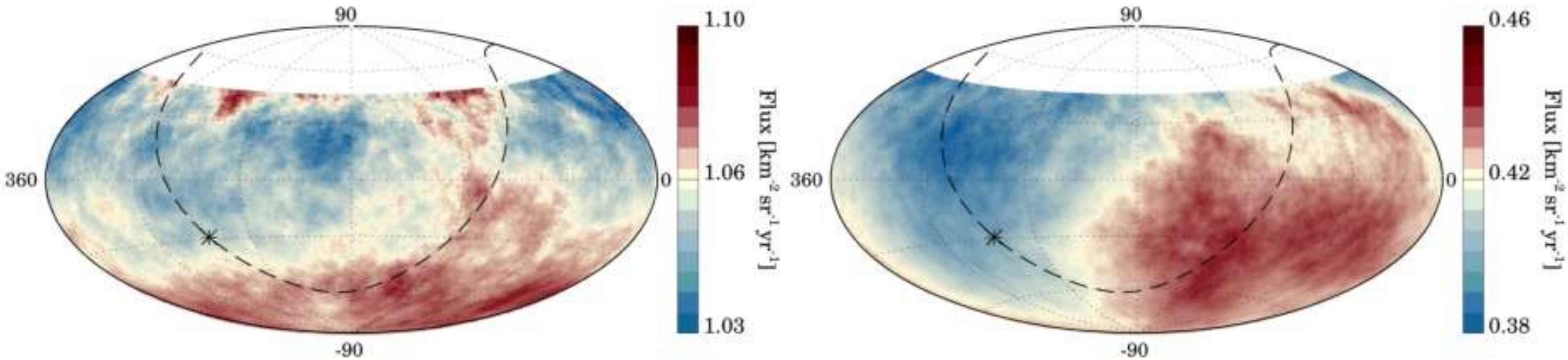

Figure 2. Maps in equatorial coordinates of the CR flux, smoothed in windows of 45°, for the energy bins [4, 8] EeV (left) and $E \geqslant 8$ EeV (right). The Galactic plane is represented with a dashed line, and the Galactic center is indicated with a star.

Table 3
Results of the First-harmonic Analysis in R.A. in the Three Bins above 8 EeV

Energy (EeV)	Events	a_1^α	b_1^α	r_1^α	φ_1^α (deg)	$P(\geqslant r_1^\alpha)$
8–16	24,070	-0.011 ± 0.009	0.044 ± 0.009	0.046	104 ± 11	3.7×10^{-6}
16–32	6604	0.007 ± 0.017	0.050 ± 0.017	0.051	82 ± 20	0.014
$\geqslant$32	1513	-0.03 ± 0.04	0.05 ± 0.04	0.06	115 ± 35	0.26

Now updated extended to higher energies

Large scale anisotropies

Dipole strenght seems to increase with energy, BUT low statistics -> low significance

THE ASTROPHYSICAL JOURNAL, 868:4 (12pp), 2018 November 20 Aab et al.

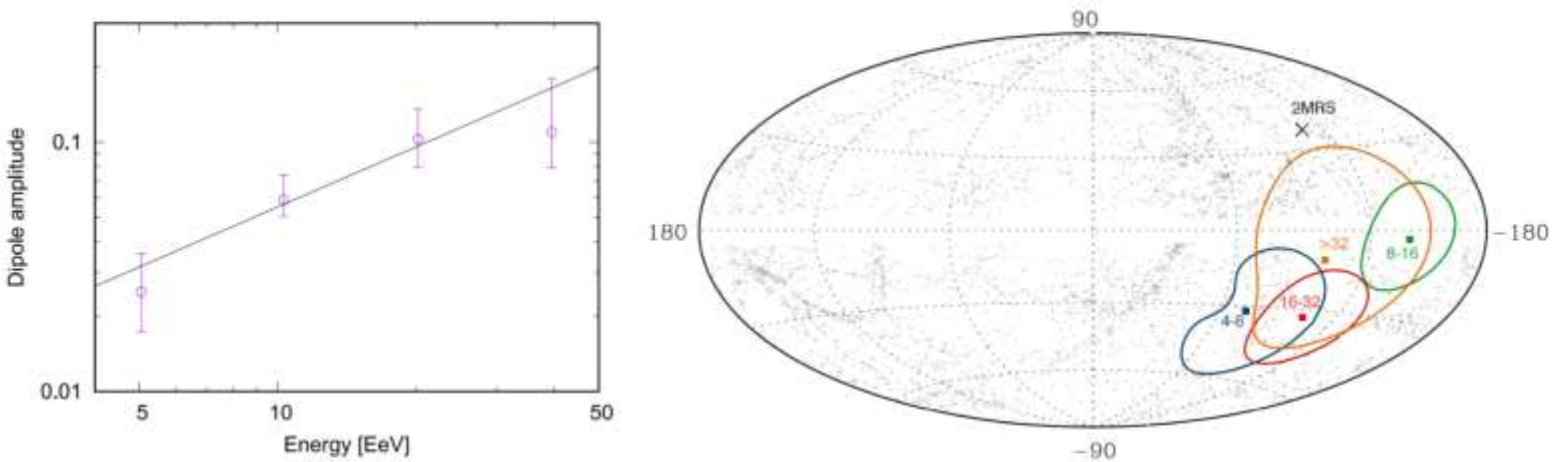

Figure 3. Evolution with energy of the amplitude (left panel) and direction (right panel) of the 3D dipole determined in different energy bins above 4 EeV. In the sky map in Galactic coordinates of the right panel the dots represent the direction toward the galaxies in the 2MRS catalog that lie within 100 Mpc, and the cross indicates the direction toward the flux-weighted dipole inferred from that catalog.

We find that the amplitude increases with energy above 4 EeV, with **a constant amplitude being disfavored at the 3.7σ level**. A growing amplitude of the dipole with increasing energies is expected owing to the smaller deflections suffered by CR at higher rigidities. The dipole amplitude is also enhanced for increasing energies owing to the increased attenuation suffered by the CR from distant sources, which implies an increase in the relative contribution to the flux arising from the nearby sources, leading to a more anisotropic flux distribution.

Large scale anisotropies

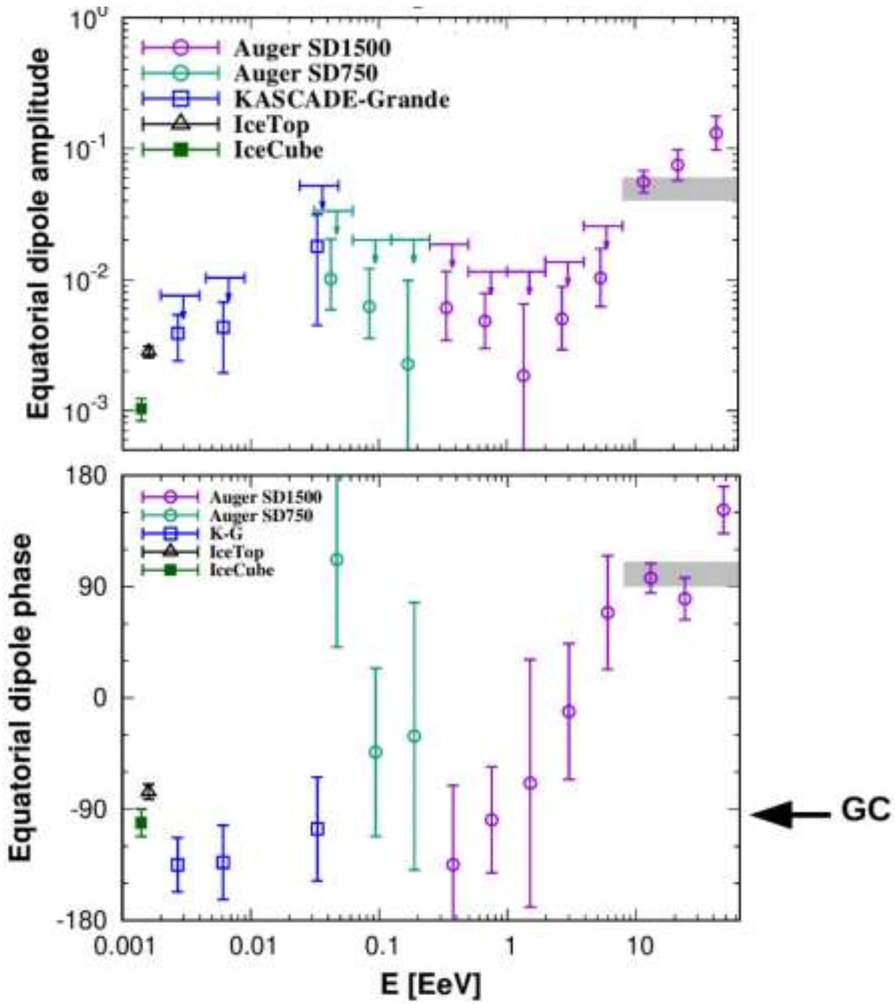

amplitudes grow, from below 1% to above 10%

phases shift, from ~GC to ~ opposite direction

Suggests transition from anisotropies of Galactic origin below ~1 EeV to extragalactic origin above few EeV

Extragalactic component could be sizeable below 1 EeV, as long as it is sufficiently isotropic

Small/intermediate scale anisotropies

Blind search - whole sky 1°x 1°grid
Scan:
$1° \leq \psi \leq 30°$
32 EeV $\leq E_{th} \leq$ 80 EeV

Most significant excess:
R.A.=202. Dec=-45.

E_{th} = 38 EeV
ψ = 27°
n_{obs} = 188 n_{exp} = 125
local Li-Ma significance=5.6σ
post-trial p-value=2.5%

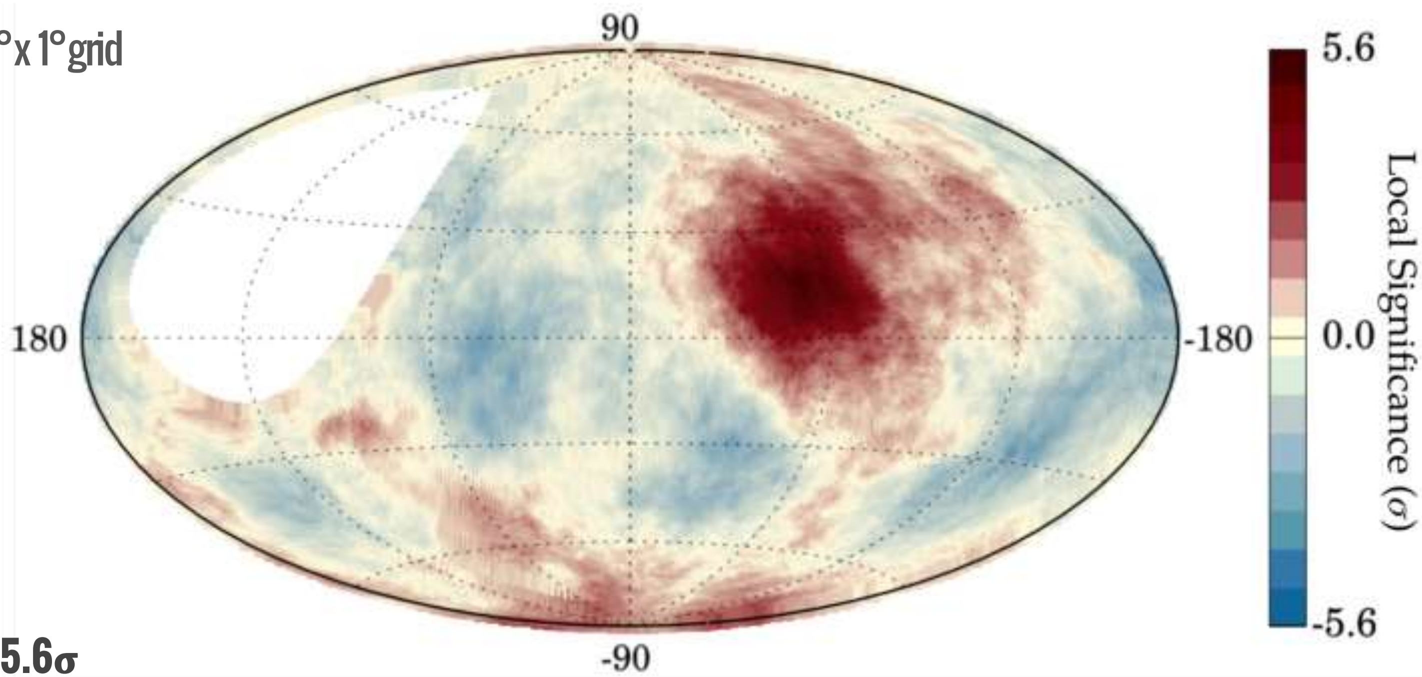

Small/intermediate scale anisotropies

Cen A is the closest radiogalaxy
D~3.6 Mpc

Scan:
$1° \leq \psi \leq 30°$
$32\ \mathrm{EeV} \leq E_{th} \leq 80\ \mathrm{EeV}$

Most significant excess:
$E_{th} = 37$ EeV
$\psi = 28°$
$n_{obs} = 203$ $n_{exp} = 141$
local p-value=$1.5\mathrm{x}10^{-7}$
post-trial : 3.9σ

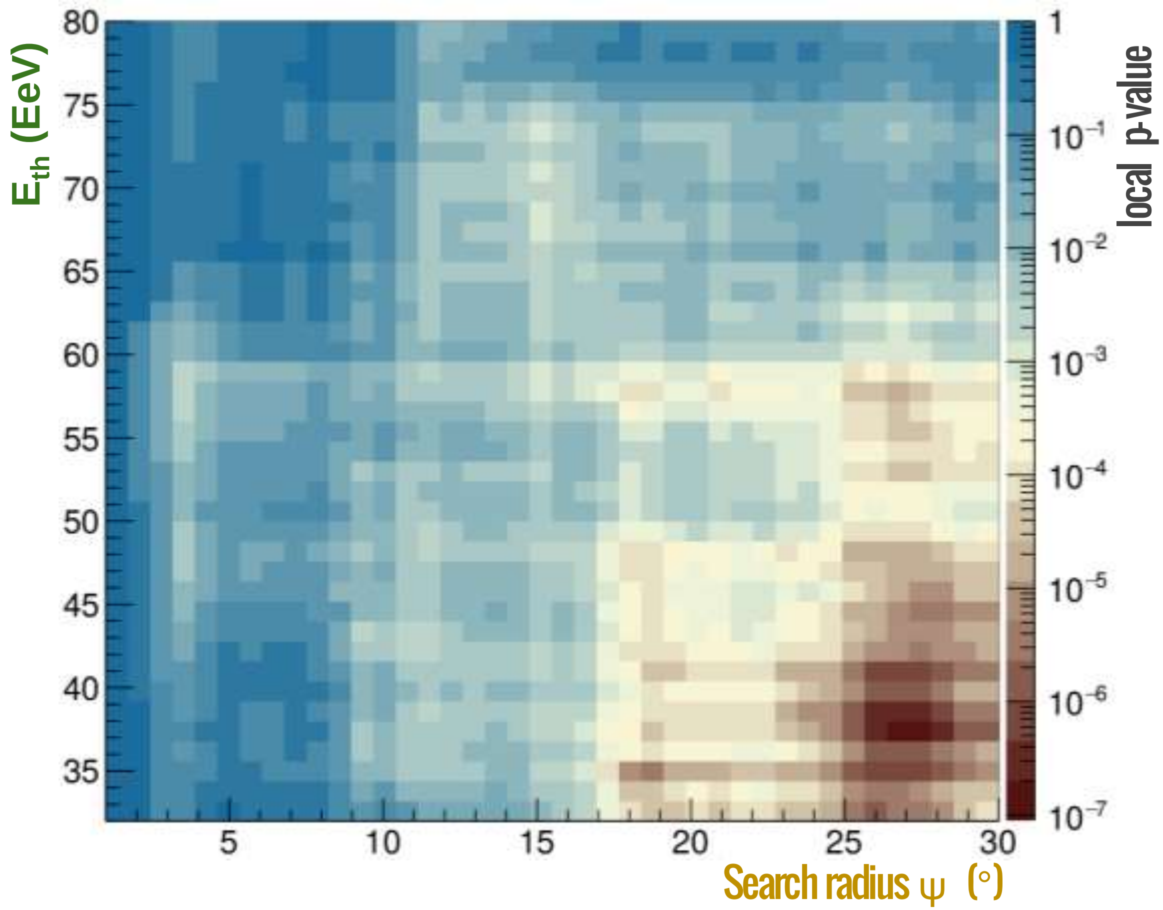

Small/intermediate scale anisotropies

We expect that **brighter** objects contribute more to the flux, and we want to take into account **interaction**:
➤ **Likelihood Method** (for details see The Pierre Auger Collaboration - ApJL, 853:L29 (2018))

Probability maps built including:

- Weight objects by their relative flux in the corresponding electromagnetic wavelength
- Different attenuation due to different distances to sources taken into account
- A smearing angle θ around each object to take into account magnetic deflections ➤ **First free parameter**
- Source fraction (rest isotropic) ➤ **Second free parameter (f_{aniso})**
- Directional exposure normalized to the total number of events

Test statistic defined as the ratio of likelihoods: $TS = 2 \operatorname{Log} [\mathscr{L}(\psi, f_{aniso})/\mathscr{L}(f_{aniso}=0)]$

Scan in energy thresholds **32 EeV ≤ Eth ≤ 80 EeV [1 EeV steps]**

Test 4 different catalogs

Small/intermediate scale anisotropies

γ-emitting AGNs

- Selected using Fermi 3FHL (was 2FHL)
- UHECR flux proxy: Φ(E>10 GeV)
- 33 sources (including Cen A, Fornax A, M87, Mkn421)
- Majority blazars of BL-Lac type and radio-galaxies of FR-I type

Swift-BAT

- UHECR flux proxy: Φ(14-195 keV)
- Different AGN sample than previous one (both radio loud and quiet)
- >300 sources

Starburst Galaxies

- UHECR flux proxy Φ(1.4 Ghz)
- Selection based on *Ackermann+ 12* and *Becker+ 09*, with the addition of data from HEASARC Radio Master Catalog
- 32 sources (including Circinus, M82 M83…)

2MRS

- UHECR flux proxy Φ(k-band)
- Traces local matter (some 10^4 sources)
- Local group taken away by selecting only events with D>1Mpc

More details about catalog selection in ApJL, 853:L29 (2018)

Small/intermediate scale anisotropies

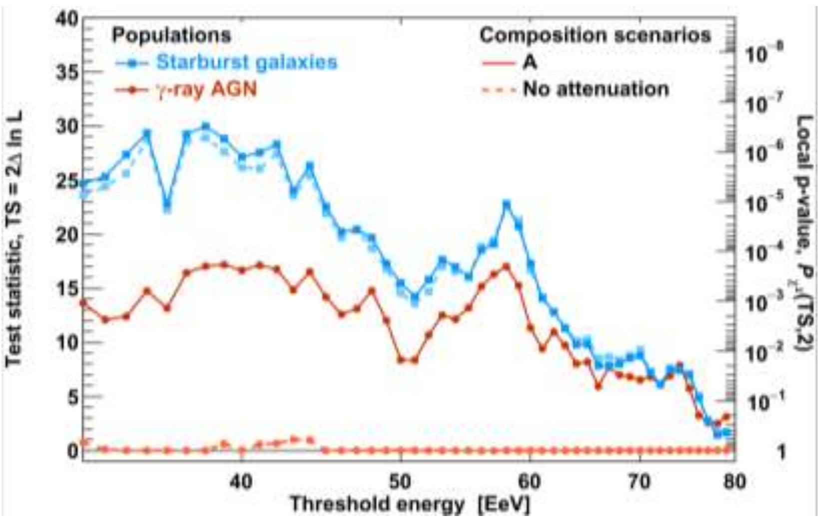

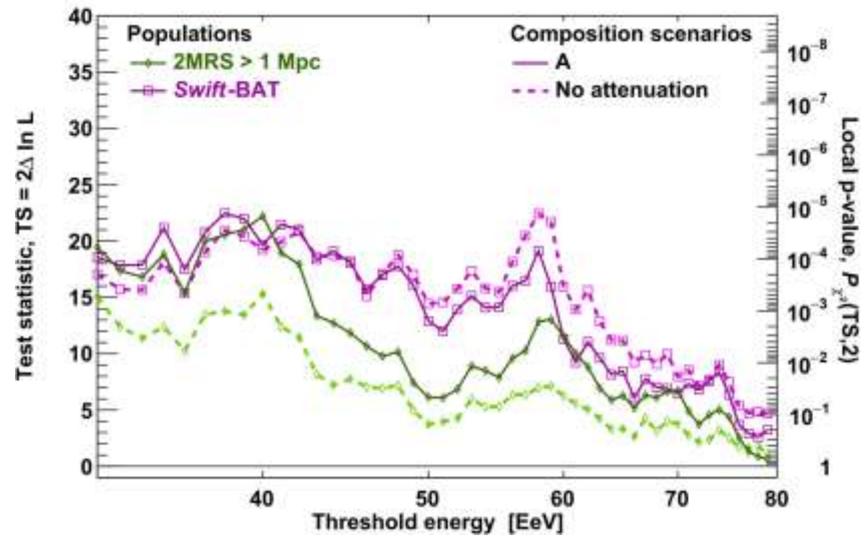

Catalog	E_{th}	θ	f_{aniso}	TS	Post-trial
Starburst	38 EeV	15^{+5}_{-4}°	11^{+5}_{-4}%	29.5	4.5 σ
γ-AGNs	39 EeV	14^{+6}_{-4}°	6^{+4}_{-3}%	17.8	3.1 σ
Swift-Bat	38 EeV	15^{+6}_{-4}°	8^{+4}_{-3}%	22.2	3.7 σ
2MRS	40 EeV	15^{+7}_{-4}°	19^{+10}_{-7}%	22.0	3.7 σ

Highest TS = 29.5 found for starburst galaxies with E_{th}=38 EeV

All the most significant excesses happen at similar E_{th} and angular scale

Note: 15° smearead Fisher-Von Misses distribution $\sim$1.59×15°=24±8° top-hat

Small/intermediate scale anisotropies

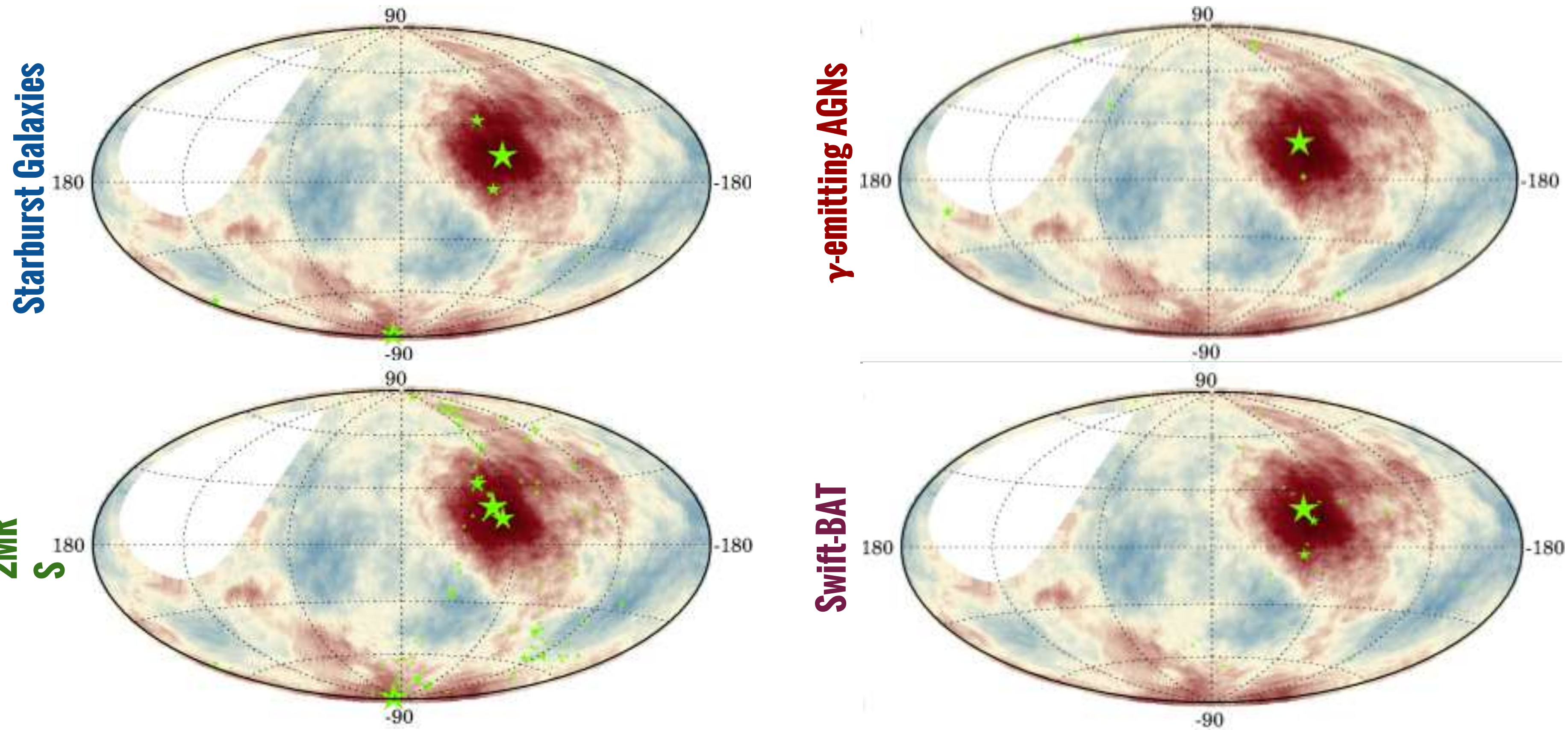

Multi-messenger astrophysics - neutrinos

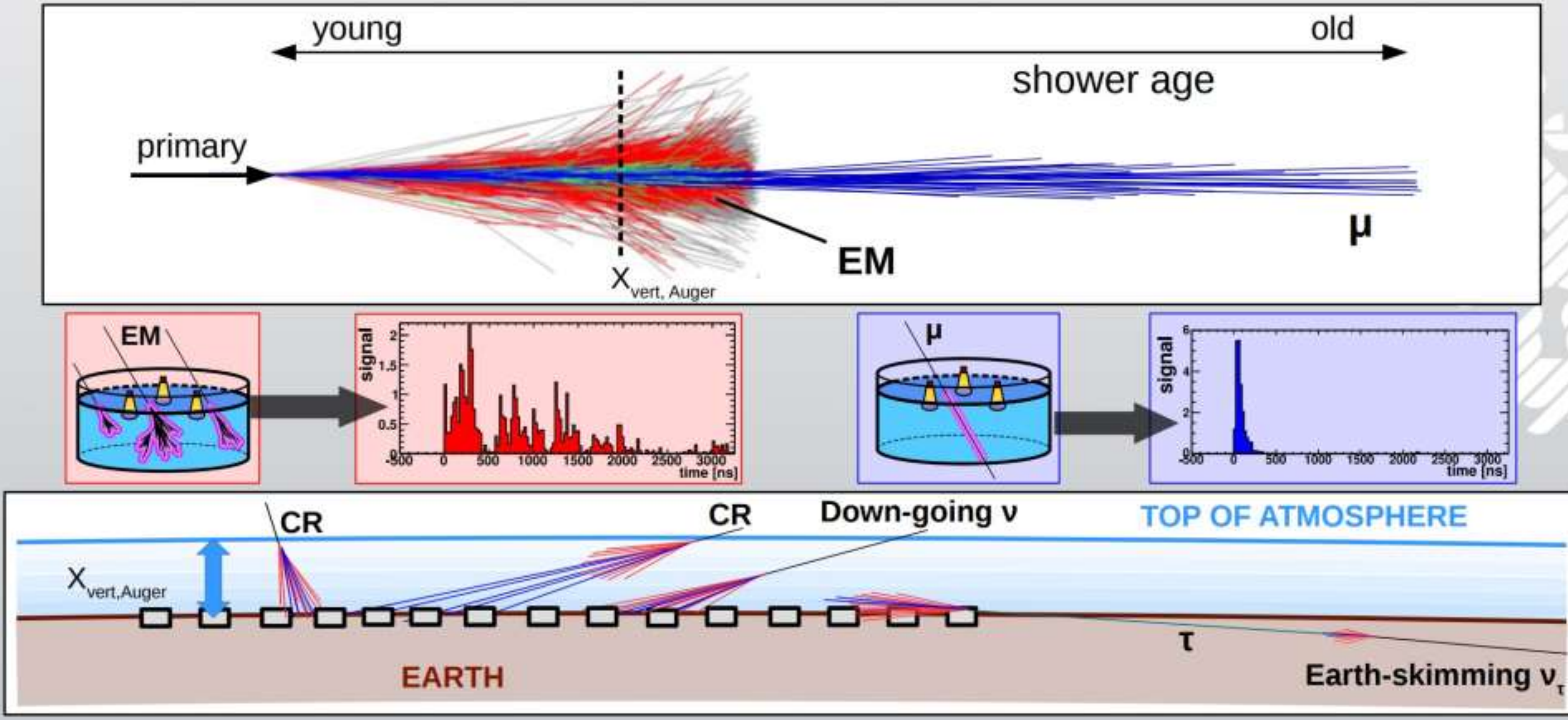

M. Schimp for the Pierre Auger Collaboration - ICRC 2019

Multi-messenger astrophysics - neutrinos

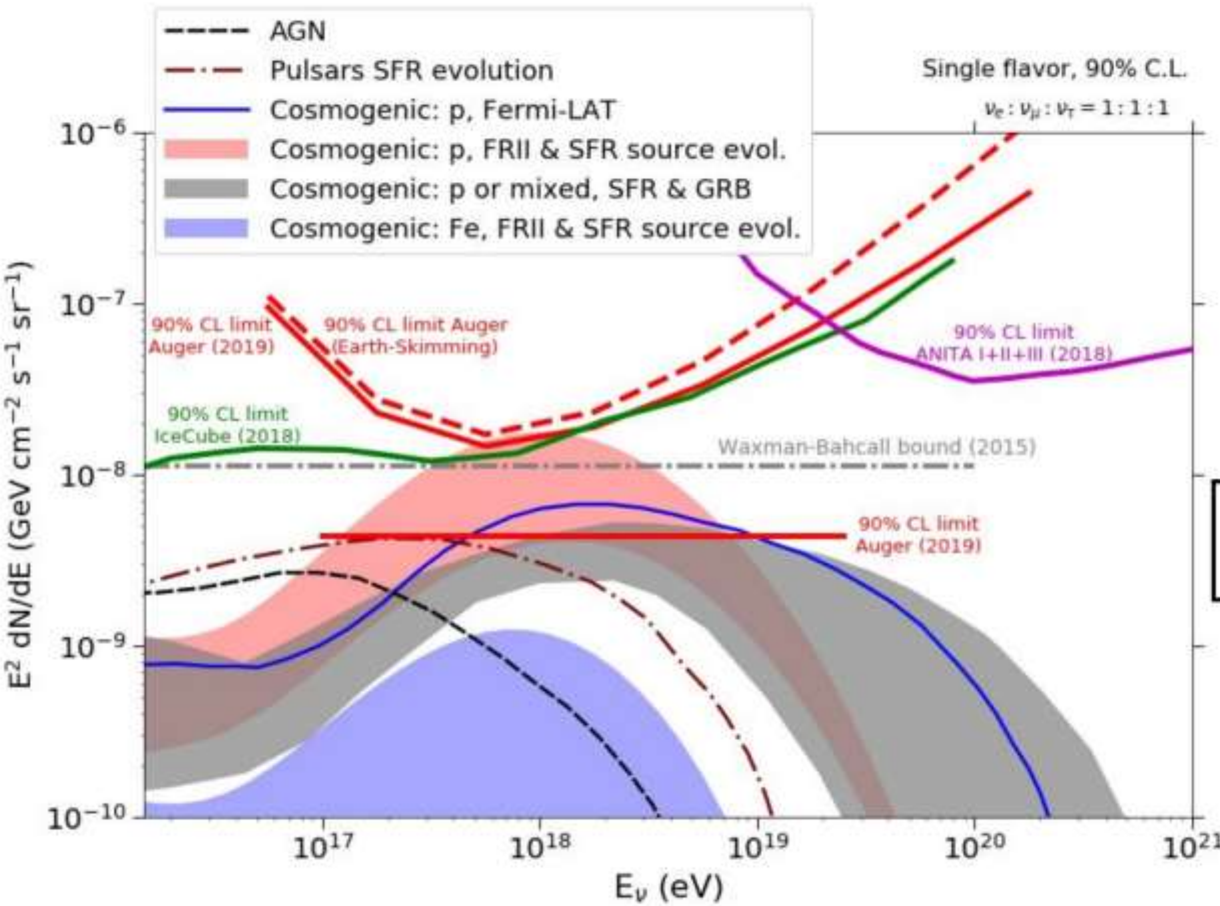

arXiv:1906.07422

Expected ν events:
Red band: 1.4 - 5.9
Gray band: 0.8 - 2.0
Blue band (top): 0.4

Auger Limit: $dN/dE = k\,E^{-2}$
$k \sim 4.4 \times 10^{-9}$ GeV cm^{-2} s^{-1} sr^{-1}

SD Data:
Jan. 2004 –
August 2018

Multi-messenger astrophysics - neutrinos

No neutrino candidate found. Limits placed (depending on declination)

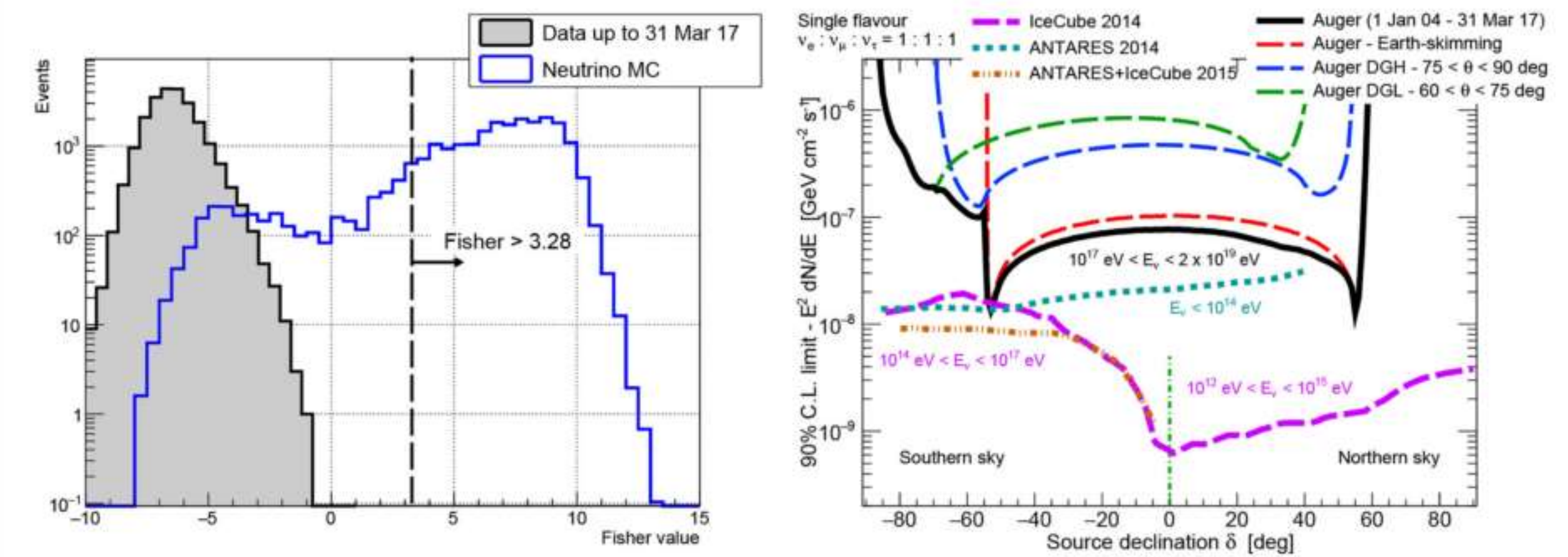

FIGURE 1 | (Left) Distribution of the Fisher variable for the DGH search (see text) for simulations compared to a small fraction of the data and assumed to be due to cosmic rays. The cut is made at a value of the Fisher variable of 3.28. **(Right)** Limits to the point source fluxes as a function of equatorial declination obtained from the non-observation of ES and DGH neutrino candidates up to March 31st 2017 (from Zas, 2018).

Multi-Messenger Physics with the Pierre Auger Observatory Front. Astron. Space Sci. 6:24 (2019)

Multi-messenger astrophysics - neutrinos

No neutrino candidate found in correlation with GW events. Limits placed (depending on declination)

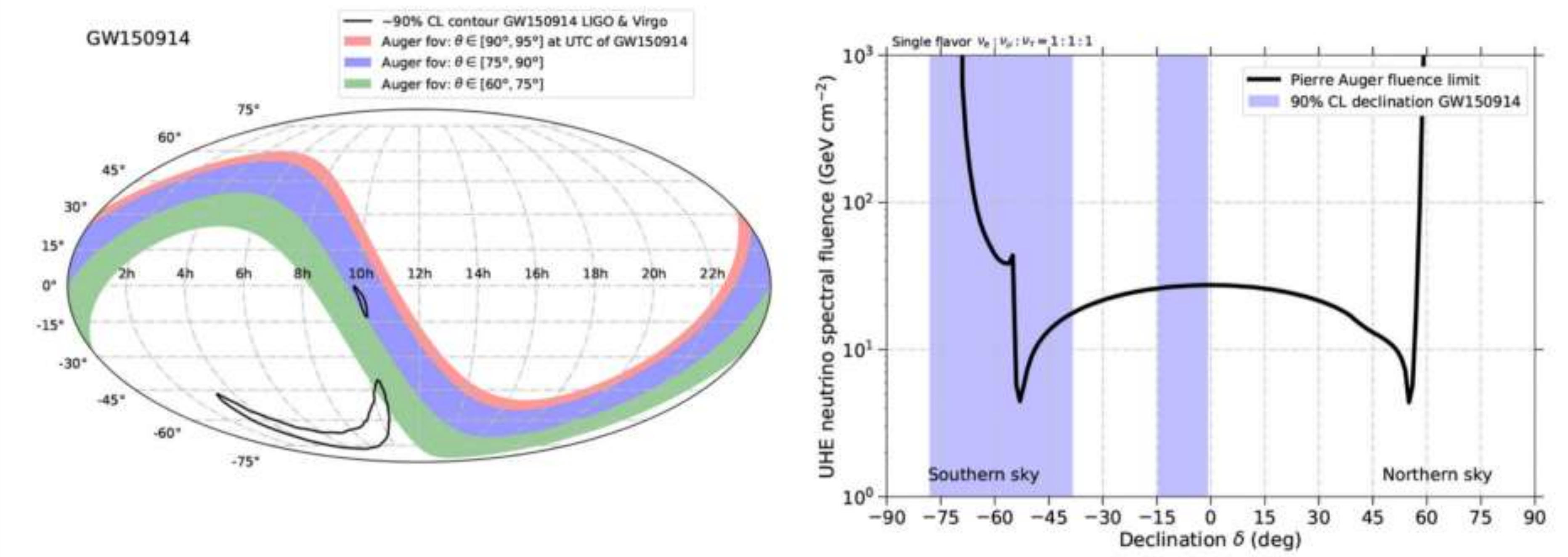

FIGURE 2 | (Left) Field of view of the Observatory exemplified at the instant of detection of the black hole coalescence event GW150914 by Advanced LIGO (LIGO-Collaboration, 2018). The band limits from top to bottom correspond to lines of zenith angles 95°, 90°, 75°, and 60°, used to separate the neutrino search into ES, DGH, and DGL channels. The black contours give the 90% C.L. region of the reconstructed position of the BH merger as obtained by LIGO observations. **(Right)** Upper limit at 90% C.L. to the neutrino spectral fluence in the 100 PeV to 25 EeV range as a function of declination (see text), for the detection of black hole merger GW150914. The blue band is the 90% C.L. of the reconstructed source declination, illustrating the limited precision level achieved using just detections at two LIGO sites.

Multi-Messenger Physics with the Pierre Auger Observatory Front. Astron. Space Sci. 6:24 (2019)

Multi-messenger astrophysics - neutrinos

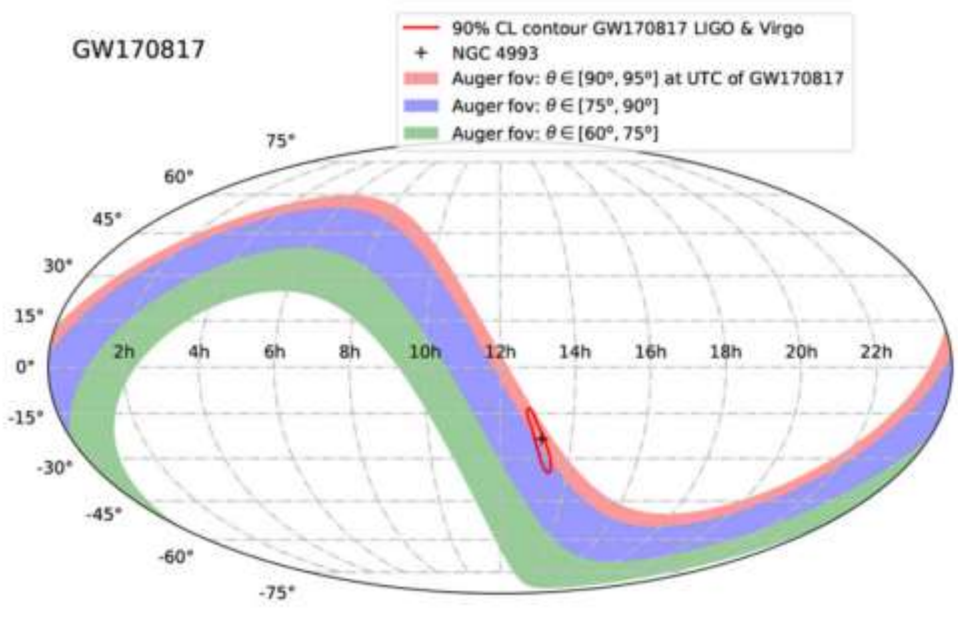

FIGURE 3 | Field of view of the Observatory in Earth-skimming and down-going channels at the instant of the detection of neutron star merger GW170817. The small red contour marks the event localization obtained by the Ligo-Virgo collaborations (LIGO-Collaboration, 2018) and the black cross is the position of NGC 4993, later correlated to the event by optical telescopes (Coulter et al., 2017).

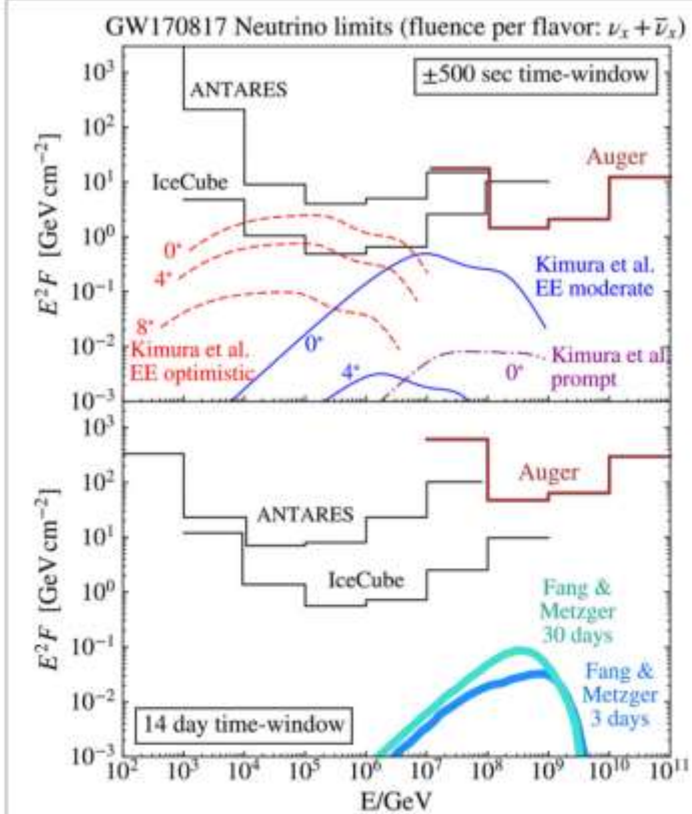

FIGURE 4 | Upper limits at 90% C.L. on the neutrino spectral fluence from GW170817 for a 1,000 s period centered at (14 day after) the time of the event in the top (bottom) panel. The bounds in the top panel are compared to predictions of models of prompt and extended emission (EE) (Kimura et al., 2017) in the case of exact alignment of the line of sight to the rotation axis and for selected off-axis viewing angles. The bounds obtained for a 14-day period on the bottom panel are compared to models of longer lived emission (Fang and Metzger, 2017). All models have been scaled to 40 Mpc, the distance to the host galaxy NGC 4993 (Modified from Albert et al., 2017a).

Limit for the NS-NS merger. We were quite lucky!

Multi-messenger Observations of a Binary Neutron Star Merger

The Astrophysical Journal Letters, 848:L12, 2017

Multi-messenger astrophysics - photons

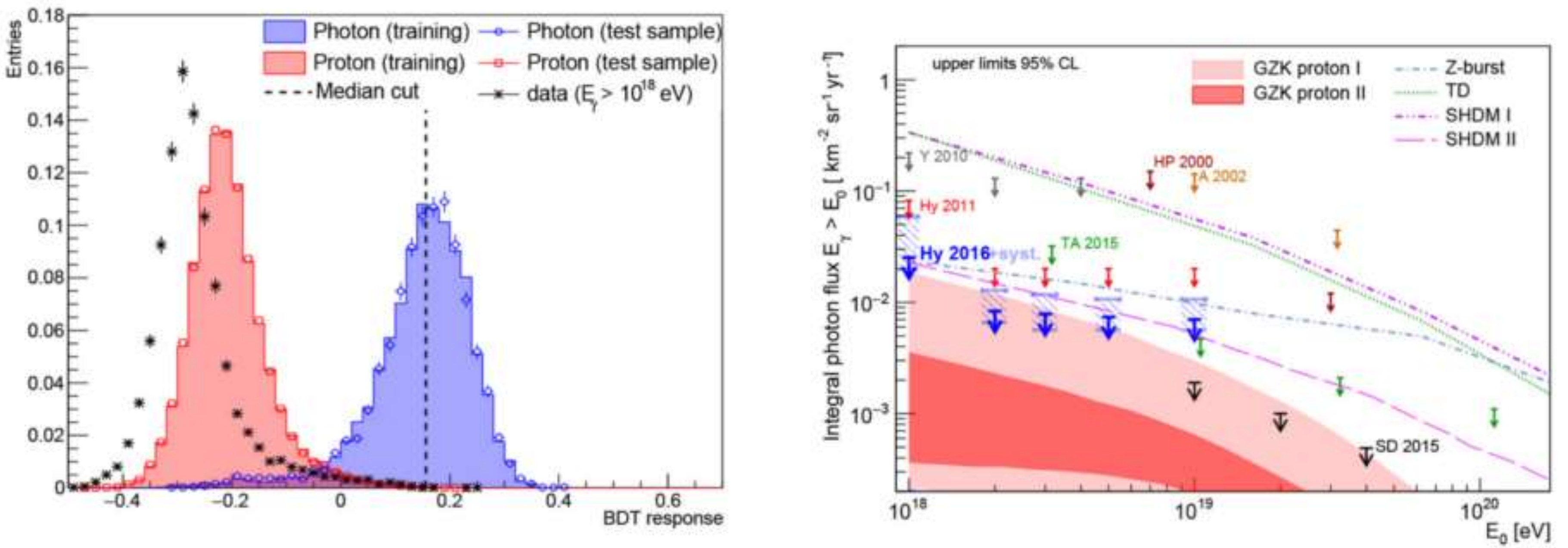

FIGURE 5 | (Left) Photon identification with a Boosted Decision Tree for signal (photon, blue), background (proton, red) and data (black). For simulations, both the training and the test samples are shown. The cut at the median of the photon distribution is indicated by the dashed line. QGSJET-II-04 is used as high-energy hadronic interaction model. **(Right)** Compilation of upper limits on the integral photon fluxes from Aab et al. (2017e). Blue arrows: Integral photon upper limits from the 9 year hybrid data sample assuming a photon flux following E^{-2} and with no background subtraction. The limits obtained when the detector systematic uncertainties are taken into account are shown as horizontal segments (light blue) delimiting a dashed-filled box at each energy threshold; Black arrows: Nine year SD data sample (Bleve, 2016). Previous data from Auger as well as data from TA, AGASA, Yakutsk, and Haverah Park are included for comparison. The lines and shaded regions give the predictions for top-down models and GZK photon fluxes, respectively, assuming different parameters (references can be found in Aab et al., 2017e).

Multi-messenger astrophysics - photons

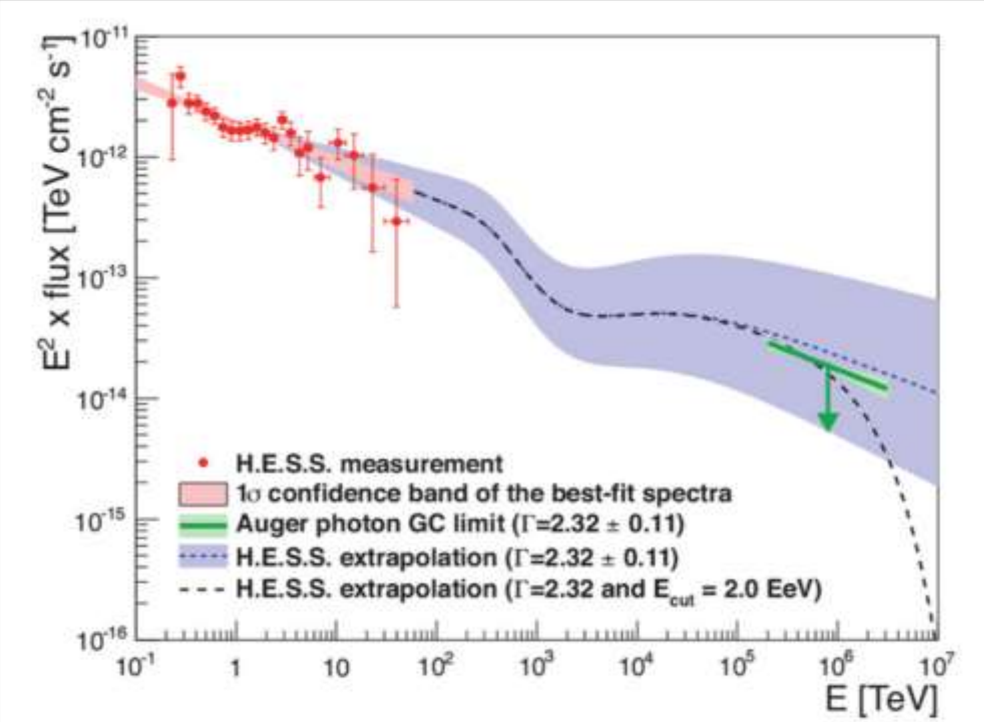

FIGURE 6 | Gamma-ray spectrum from the Galactic center region as measured by the H.E.S.S. collaboration (red points) (Abramowski et al., 2016). The measured photon flux is extrapolated into the EeV range, given the quoted spectral index and its uncertainties (blue shaded region). The Auger limit (Aab et al., 2017a) is indicated by a green line (the green band reflects again the spectral uncertainties of the gamma-ray spectrum). A spectral index with cutoff energy $E_{cut} = 2.0 \cdot 10^6$ TeV is indicated by the dashed line.

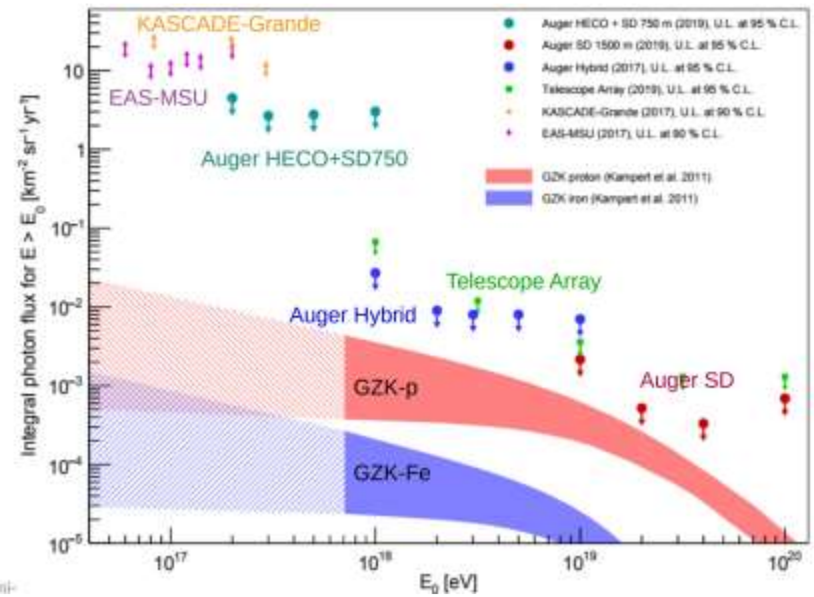

J. Rautenberg for the Pierre Auger Collaboration - ICRC 2019

Search for neutrino-UHECR correlation

$p + \gamma/p \longrightarrow \pi^{+} + n$

Neutrons can be produced in the proximity of the source

- Decay lenght is about $\simeq$ 9.2 (En/EeV) kpc -> they can reach us from Galactic sources
- Neutron-induced showers are indistinguishable from proton-induced ones
- -> need to look for localized excesses

Results for the Most Significant Target from Each Target Set

Class	R.A. [°]	Decl. [°]	Obs	Exp	Flux U.L. (km^{-2} yr^{-1})	E-Flux U.L. (eV cm^{-2} s^{-1})	*p*-value	*p*-value (penalized)
msec PSRs	260.27	−24.95	237	214	0.019	0.14	0.058	0.98
γ-ray PSRs	8.59	−5.58	176	149	0.024	0.18	0.016	0.70
LMXB	264.57	−26.99	265	219	0.028	0.20	0.0012	0.10
HMXB	152.45	−58.29	283	248	0.019	0.14	0.014	0.49
H.E.S.S. PWN	128.75	−45.60	275	248	0.018	0.13	0.043	0.53
H.E.S.S. other	269.72	−24.05	235	211	0.019	0.14	0.054	0.59
H.E.S.S. UNID	266.26	−30.37	251	227	0.018	0.13	0.055	0.57
Microquasars	262.75	−26.00	247	216	0.022	0.16	0.020	0.23
Magnetars	81.50	−66.08	268	241	0.016	0.11	0.040	0.48
Gal. center	266.42	−29.01	234	223	0.014	0.10	0.24	...
Gal. plane	|Gal. lat.| < 1°17		16965	17197	0.077	0.56	0.96	...

Search at different energy thrensolds, results from The Pierre Auger Collaboration, ApJ, 789 (2014) L34

Search for neutrino-UHECR correlation

$p + \gamma/p \longrightarrow \pi^{+} + n \longrightarrow \mu^{+} + \nu_{\mu} + n \longrightarrow e^{+} + \overline{\nu}_{\mu} + \nu_{e} + \nu_{\mu} + n$

$\longrightarrow \pi^{0} + p \longrightarrow \gamma + \gamma + p$

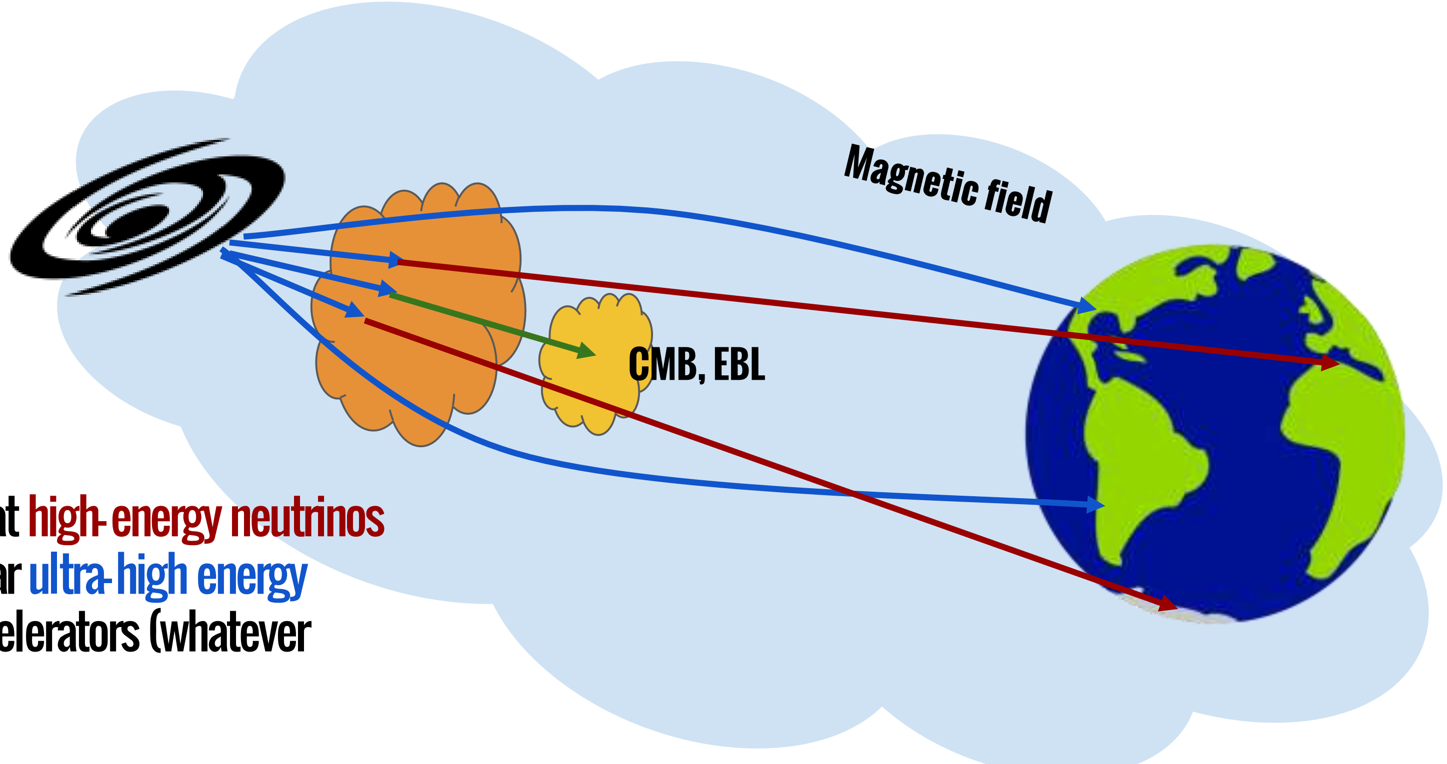

It is expected that high-energy neutrinos are produced near ultra-high energy cosmic rays accelerators (whatever they may be)

Search for neutrino-UHECR correlation

- WG presented at UHECR 2014 originally with IceCube, Telescope Array and Auger
  - in 2017 ANTARES enters the WG.
- First results presented at ICRC 2015 and published in JCAP 1601 (2016) 01, 037.
- Updated at ICRC 2017 with new neutrino data from IceCube and 1 more year of TA data

Three analyses:

1) Cross-correlation method using the high-energy cascades and the high-energy tracks
2) Likelihood method stacking the high-energy cascades and the high-energy tracks
3) Likelihood method stacking UHECRs and using the neutrino point source sample

- In the first publication, potentially interesting results were found in the analyses done between UHECR and high-energy cascades. These p-values have become larger with more statistics.
- Updated results was presented at UHECR 2018 and ICRC 2019 with new data from Auger, TA and data from ANTARES for the first time.
  The p-values for cascades have increased up to $\sim 2.7 \times 10^{-2}$
- See also L. Caccianiga for the 4 collaborations, http://arxiv.org/abs/1905.03997

The Pierre Auger Observatory - Auger Prime

The **Future** is here: **Auger Prime**

Major upgrade of the detector:

- **Faster** electronics
- **Scintillators** on top of (almost) each WCD
- a fourth, **smaller PMT** to extend dynamic range
- **radio** antennas on (almost) each WCD
- Extended FD operation to periods with higher night sky background to have more statistics

Deployment already started

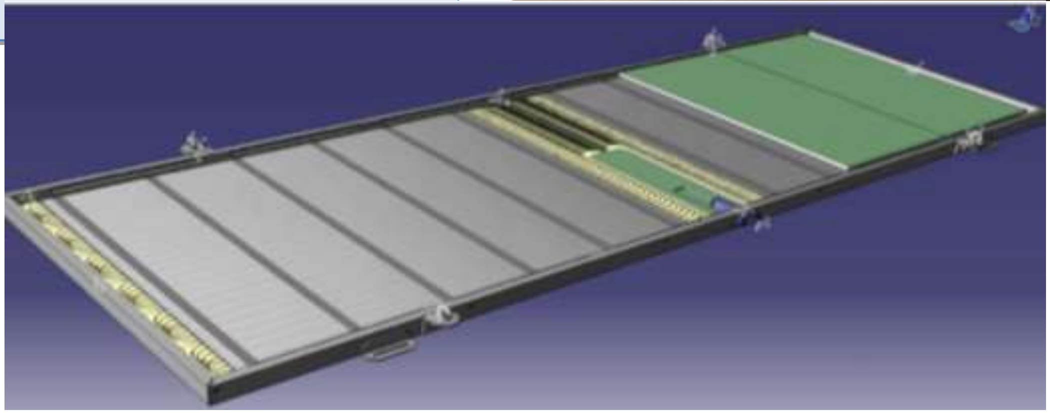

The Pierre Auger Observatory - Auger Prime

$$\begin{pmatrix} S_{\mathrm{SSD}} \\ S_{\mathrm{WCD}} \end{pmatrix} = \begin{pmatrix} \lambda\,\mathcal{A}_{\mathrm{SSD}} & \mathcal{A}_{\mathrm{SSD}} \\ \beta\,\mathcal{A}_{\mathrm{WCD}} & \mathcal{A}_{\mathrm{WCD}} \end{pmatrix} \begin{pmatrix} \mathcal{F}_{\mathrm{em}} \\ \mathcal{F}_{\mu} \end{pmatrix}$$

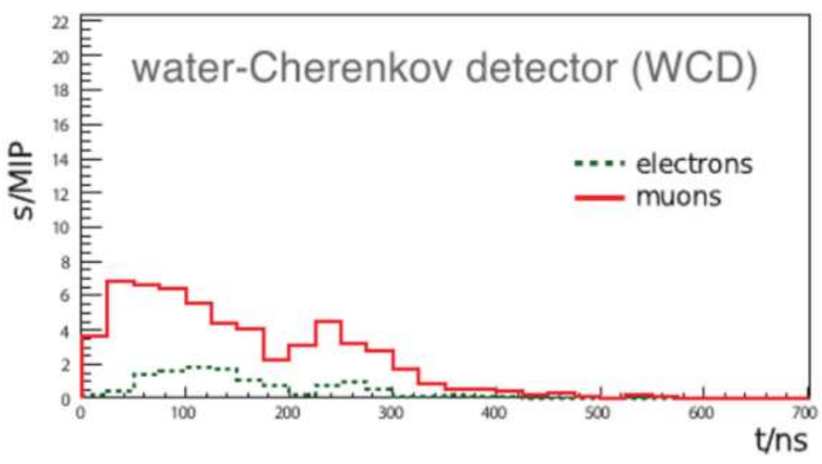

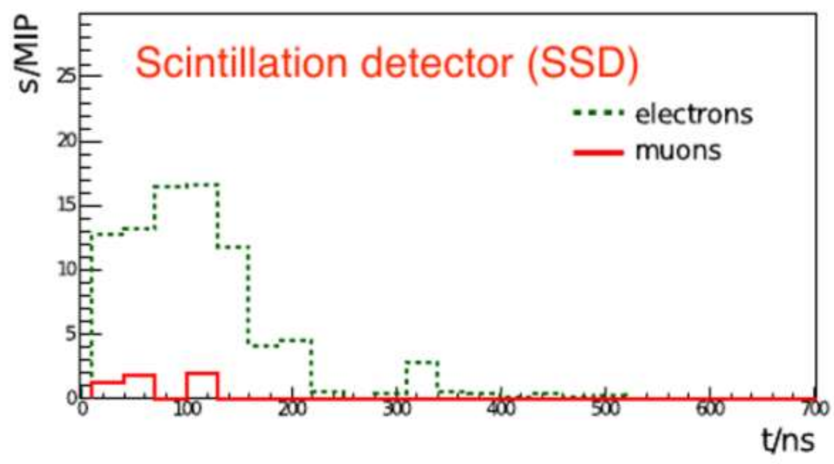

The Pierre Auger Observatory - Auger Prime

SSD will mostly be efficient for vertical showes: for horizontal showers radio will be exploited

AERA detector (small area and small spacing) already operational inside Auger

-> Extend to the whole array

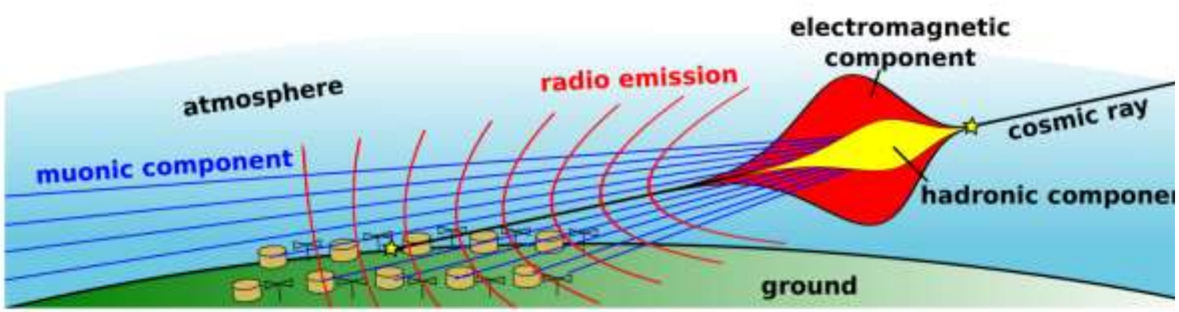

Figure 7. Sketch of a horizontal air shower. The electromagnetic as well as the hadronic air shower components are absorbed i atmosphere and only muons penetrate to the detectors. The atmosphere is transparent to radiation with frequencies in the 30 – 80 MHz band. (courtesy Ewa Holt)

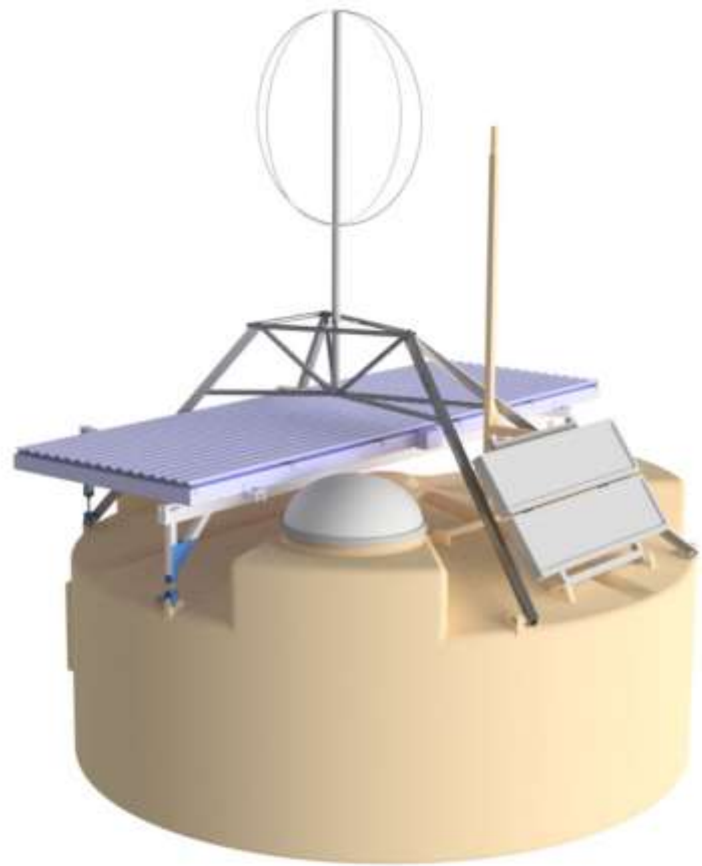

Thank you for your attention!

Backup slides

Discussion

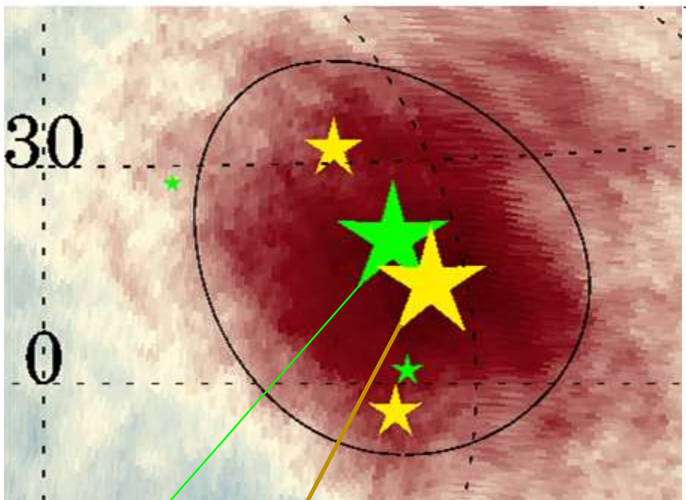

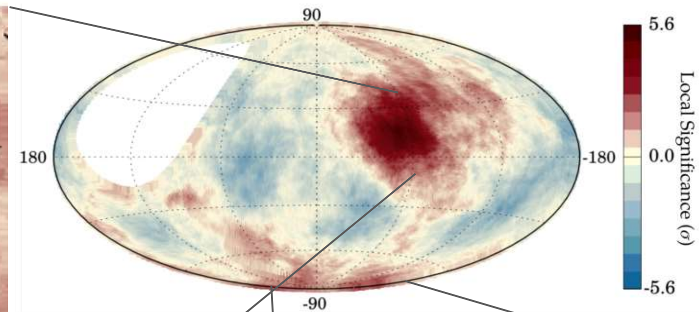

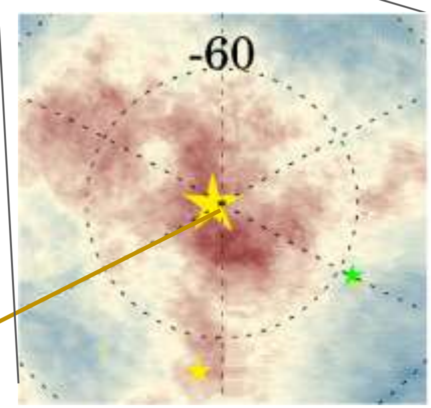

Cen A

Most contributing source to 2MRS, γ-AGNs and Swift-BAT

NGC 4945

Most contributing source to starburst

NGC 253

2nd-most contributing source to starburst

Evolution in time

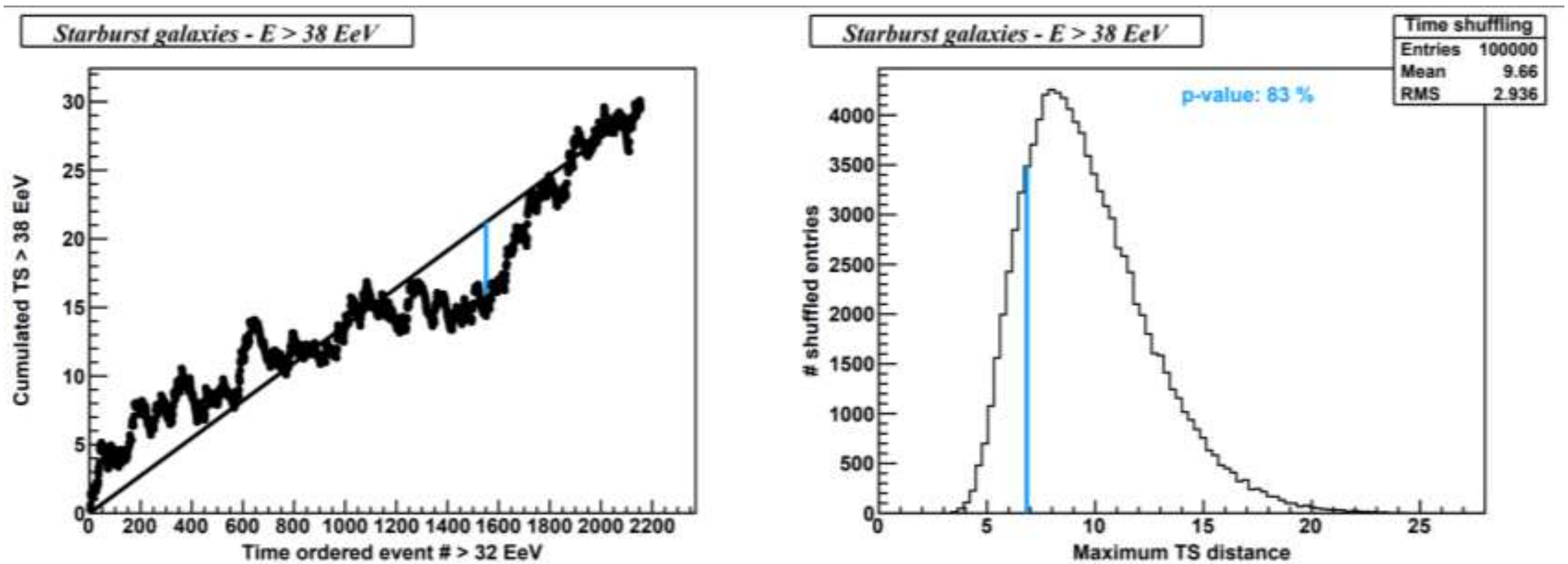

Model Excess Map

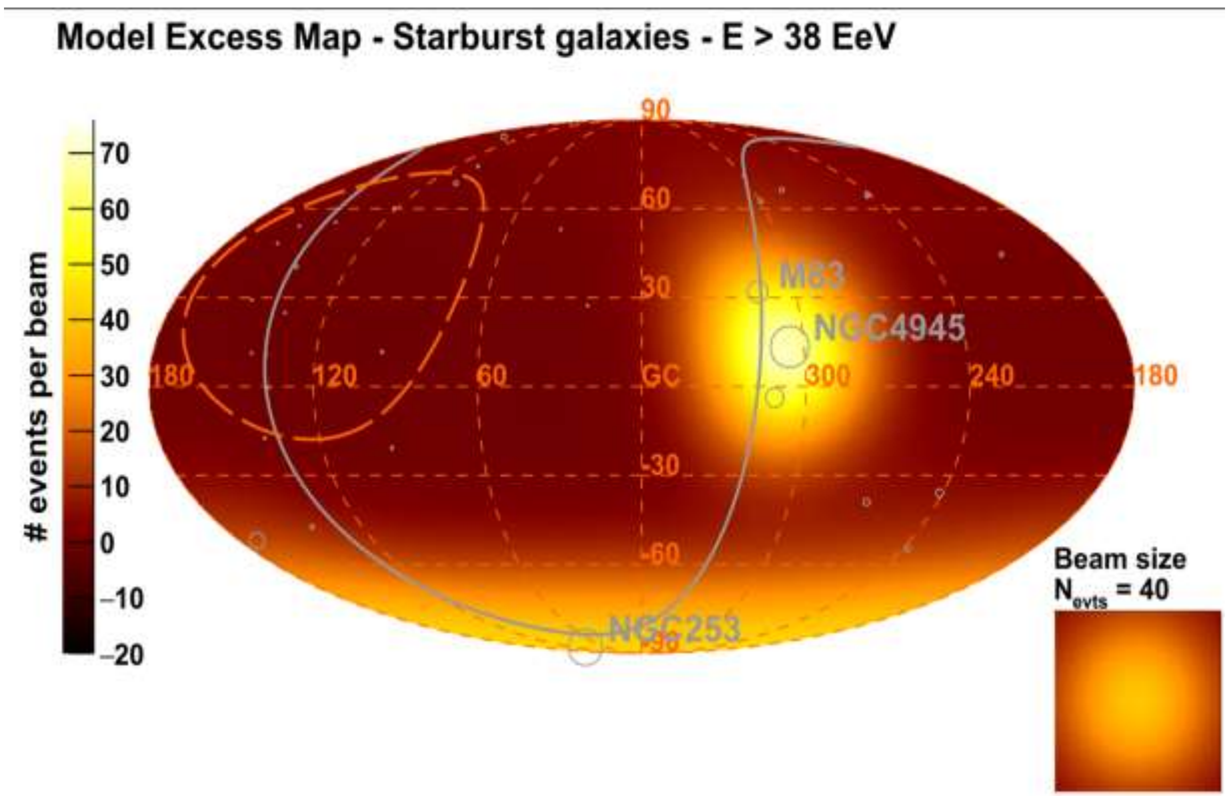

Parameter space